www.sciencemag.org/cgi/content/full/science.aao1710/DC1

Supplementary Materials for

A major chromatin regulator determines resistance of tumor cells to T cell–mediated killing

Deng Pan,* Aya Kobayashi,* Peng Jiang,* Lucas Ferrari de Andrade, Rong En Tay, Adrienne Luoma, Daphne Tsoucas, Xintao Qiu, Klothilda Lim, Prakash Rao, Henry W. Long, Guo-Cheng Yuan, John Doench, Myles Brown, Shirley Liu,† Kai W. Wucherpfennig†

*These authors contributed equally to this work.
†Corresponding author. Email: kai_wucherpfennig@dfci.harvard.edu (K.W.W); xsliu@jimmy.harvard.edu (S.L.)

Published 4 January 2018 on *Science* First Release
DOI: 10.1126/science.aao1710

This PDF file includes:

Materials and Methods
Figs. S1 to S15
Tables S1 to S5
References

Materials and Methods

Cell Culture

B16F10 cells were maintained in complete DMEM media (10% FBS and 50U/ml of Penicillin-Streptomycin). B16F10-Cas9 cells were maintained in complete DMEM media with 2.5-5ug/ml of blasticidin. CD8 T cells isolated from mice were cultured in complete RPMI 1640 media (10%FBS, 20mM HEPES, 1mM sodium pyruvate, 0.05mM 2-mercaptoethanol, 2mM L-glutamine and 50U/ml streptomycin and penicillin).

Generation of murine B16F10-Cas9 cell lines

Lentiviral Cas9-Blast (Addgene #52962) vector was co-transfected with packaging plasmids pCMV-dR8.91 and pCMV-VSV-G (Addgene #8454) into HEK293T cells. Transfection was performed using TransIT-293 (Mirus, MIR2700) following the manufacturer's protocol. Virus was harvested at 48 hours post-transfection, titered and stored at -80°C. B16F10 cells were infected with Cas9-Blast lentivirus overnight. Two days later, infected cells were selected with 5μg/ml of blasticidin (Life Technologies R21001).

To acquire clones with high Cas9 activity, B16F10-Cas9 cells were single-cell sorted into 96-well plates. Multiple clones were infected with a lentivirus driving expression of a gRNA specific for *Cd274* and mCherry. Ten days post infection, each individual clone was stimulated with 10ng/ml of IFNγ for 24 hours, and the expression of PD-L1 was determined by FACS using an anti-Cd274 antibody (clone 10F.9G2, BioLegend, #124311). Cas9 editing efficiency was assessed by measuring the percentage of PD-L1 negative cells in the transduced ($mCherry^+$) population. Clone4, which showed an editing efficiency of >95% was selected for the subsequent screen.

Isolation and *in vitro* activation of CD8 T cells

Pmel-1 and OT-I TCR transgenic mice were purchased from Jackson Laboratory (stock # 005023 for Pmel-1 and 003831 for OT-1). CD8 T cells were isolated from spleen and lymph nodes from Pmel-1 or OT-I TCR transgenic mice using the EasySep mouse CD8+ T cell isolation kit (STEMCELL #19753) according to the manufacturer's protocol. Freshly isolated CD8 T cells were stimulated with anti-CD3/CD28 beads (Thermo Fisher Scientific #11452D) at a bead to cell ratio of 1:2. On day 3, recombinant mouse IL-2 (Biolegend, #575406) was added to the culture at 20ng/ml. T cells were used for co-culture with B16F10 cells after at least 6 days of *in vitro* activation.

Development of screening system

We generated two positive control B16F10-Cas9 cell lines for optimizing the screening system: (1) Positive control for resistance to T cell mediated cytotoxicity: $B2m^{-/-}$ (GFP^+) B16F10-Cas9 cells, and (2) Positive control for sensitization to T cell mediated killing: $Cd274^{-/-}$ ($mCherry^+$) B16F10-Cas9 cells. Positive controls were mixed with parental B16F10-Cas9 cells to achieve a frequency of ~1% for $B2m^{-/-}$ and ~10% for $Cd274^{-/-}$ cell populations. For optimization of selection, these cell populations were co-cultured with *in vitro* activated OT-I or Pmel-1 CD8 T cells at different experimental conditions. For selection with OT-I T cells, B16F10 cells were pulsed with Ova (SIINFEKL) peptide (1ng/ml) at 37◦C for 2 hours prior to co-culture with T cells. For optimal killing by Pmel-1 T cells, B16F10 cells were pretreated with 10ng/ml of IFNγ for 24 hours to enhance surface MHC class I expression (which is very low in

the absence of IFNγ) prior to co-culture with T cells. After selection for 1-3 days, tumor cells were detached from plates and the percentage of *B2m*$^{-/-}$ (GFP^{+}) and *Cd274*$^{-/-}$ (mCherry^{+}) cells was determined by FACS following gating on the DAPI^{-} CD45^{-} CD3^{-} population. Fold enrichment and depletion was calculated by comparing the ratio of positive control cells to parental cells before and after selection.

Genome-scale CRIPSR-Cas9 screen in B16F10 cells

1. gRNA pool library production: Mouse CRISPR Brie lentiviral pooled libraries consisting of 79,637 gRNAs were co-transfected with packaging plasmids (psPAX2 #12260 and pCMV-VSV-G #8454) into HEK293T cells using LT-1 transfection reagent (Mirus Cat# MIR2305) following the manufacture's protocol. Library DNA (37μg), psPAX2 DNA (46μg) and VSV-G DNA (4.62μg) was mixed and transfected into HEK293T cells in a T162 flask. Six hours after transfection, media was removed and replaced with 60ml of virus production media (DMEM media supplemented with 20% of FBS). Forty-eight hours after transfection, lentiviral media was harvested and stored in -80◦C.

2. Virus titer determination: 1x10^{6} B16F10-Cas9 cells were plated per well of a 6-well plate. B16F10 cells were infected with different amounts of lentivirus overnight in the presence of 8μg/ml of polybrene. The next day, 10^{5} infected B16F10 cells from each condition were seeded per well into a 6-well plate (in duplicates). Twenty-four hours following infection, puromycin (1μg/ml) was added. Forty-eight hours later (after uninfected cells had died), infected cells in each well were counted. We calculated the percentage of cell survival for each viral concentration using the following formula (*39*):

$$Psurvival = \frac{Cell\#\ with\ puromycin}{Cell\#\ without\ puromycin} \times 100$$

MOI(m) was calculated using following formula:

$$p_{survival} = P(n > 0) = 1 - P(n = 0) = 1 - e^{-m}$$

Single gRNA infection (SIP) rate was calculated using the following formula:

$$SIP = \frac{(1 - P_{survival})\, ln(1 - P_{survival})}{P_{survival}}$$

The MOI for screen was 0.06, which corresponds to a SIP rate of >95%.

3. Pmel1 screen: B16F10-Cas9 (clone4) cells were infected with "Brie" lentivirus at a MOI of 0.06 and cells selected with puromycin for at least 10 days prior to use in co-cultures with T cells. B16F10 cells were pretreated with 10ng/ml of IFNγ for 24 hours prior to co-culture with Pmel-1 T cells to increase MHC class I expression. A total of approximately 8 x 10^{7} B16F10 cells were prepared for each of three replicates for the Pmel-1 screen: (1) 4x10^{7} B16F10 cells were harvested for genomic DNA isolation prior to the screen; (2) 1x10^{7} B16F10 cells were co-cultured with control OT-I T cells at a 1:1 ratio (control condition, OT-I T cells were not stimulated because B16F10 cells were not pulsed with Ova peptide); (3) 1x10^{7} B16F10 cells were co-cultured with Pmel-1 T cells at a 1:1 ratio (experimental condition). B16F10 cells and T cells were co-cultured in T162 flasks for three days, and T cells were then removed by gentle

washing of the adherent tumor cells. Genomic DNA was isolated from cells regrown after T cell removal using Blood & Cell Culture DNA Maxi/Midi Kit (Qiagen #13362,13343) following the manufacturer's protocol. The Genetic Perturbation Platform at the Broad Institute of MIT and Harvard (Cambridge, MA) performed PCR amplification of the gRNA cassette for Illumina sequencing of gRNA representation. Protocols for PCR and Illumina sequencing are available online (http://portals.broadinstitute.org/gpp/public/resources/protocols).

4. OT-I screen: For the OT-I screen, B16F10 cells were pulsed with 1ng/ml of Ova peptide (SIINFEKL) at 37°C for 2 hours prior to co-culture with OT-I T cells. A total of approximately 3 x 10^8 B16F10 cells were prepared for each of three replicates for the OT-I screen: (1) $8x10^7$ B16F10 cells were harvested for genomic DNA isolation prior to the screen; (2) $9x10^7$ non-pulsed B16F10 cells were co-cultured with OT-I T cells at a 1:1 ratio (control condition, no SIINFEKL peptide pulse); (3) $9x10^7$ SIINFEKL pulsed B16F10 cells were co-cultured with OT-I T cells at a 1:1 ratio (experimental condition). Given that killing of tumor cells by OT-I was rapid, B16F10 and OT-I T cells were co-cultured for one day before T cells were removed from the culture. Genomic DNA was extracted from cells regrown following T cell removal, and the gRNA cassette was sequenced as described above.

5. Screening data analysis: For candidate gene discovery, the normalized gRNA count table was loaded into MaGeCK (Model-based Analysis of Genome-wide CRISPR-Cas9 Knockout) (*40*) by comparing the experimental and control conditions described above. Top genes were determined based on mean log2 fold change (LFC) for all gRNAs and false discovery rate (FDR). To identify significant pathways enriched or depleted in the screen, hypergeometric distribution statistics was used for computing overlapped genes sets with top positively selected or negative selected genes (|LFC|>2 and FDR<0.05). Genes included in each pathway were based on MSIgDB (Molecular signature database), http://software.broadinstitute.org/gsea/msigdb/search.jsp) and relevant literature.

Validation screen

Top hits were selected from the genome-scale screen for validation based on the following criteria: (1) |LFC| > 2, (2) FDR<0.05, and (3) known human homologs. The mini-pool gRNA library was synthesized by the Genetic Perturbation Platform at the Broad Institute and included 1,878 gene-targeting gRNAs (6 gRNAs/gene) and 2,000 control gRNAs for data normalization. Lentivirus for the mini-pool gRNA library was produced as described above, and a low MOI was used for the validation screen (MOI=0.08). Pmel-1 and OT-I screens were performed as described for the genome-scale screen with a representation (cell number/gRNA) of >5,000. For both Pmel-1 and OT-I screens, B16F10 cells and T cells were co-cultured for 3 and 1 days respectively, before T cells were removed from the culture. An Ova peptide concentration of 0.1ng/ml was used in the validation screen with OT-I T cells. Genomic DNA was extracted from cells regrown after T cell removal, and gRNA representation was quantified as described above.

In vitro validation of genes of the PBAF complex

gRNA sequences targeting *Arid2*, *Brd7* and *Pbrm1* were cloned into a PLKO3G-GFP vector and confirmed by sequencing. gRNA constructs were co-transfected with pCMV-dR8.91 and pCMV-VSV-G (Addgene #8454) into HEK293T cells. Transfection was performed using TransIT-293 (Mirus, MIR2700) following the manufacturer's protocol. Virus was harvested 48

hours later and stored at -80◦C. B16F10-Cas9 cells (clone4) were infected with a lentivirus driving expression of a single gRNA overnight to inactivate *Arid2*, *Brd7* or *Pbrm1* genes individually. Infected cells were sorted based on GFP expression by BD FACS Aria II.

For *in vitro* validation, *Arid2*, *Brd7* or *Pbrm1*-deficient B16 cells (GFP positive) were mixed with control B16F10 cells (GFP negative) at a 1:1 ratio. These cells were stimulated with 10ng/ml of IFNγ for 24 hours and then co-cultured with *in vitro* activated Pmel-1 T cells at different effector to target ratios in a 6-well plate (triplicate conditions for each gRNA). After a three-day co-culture with T cells, fold depletion of mutant B16F10 cells in the presence or absence of T cells was determined by FACS, comparing the percentage of mutant cells (GFP positive) to control B16F10 cells (GFP negative).

Western blot analysis of mutant cell lines

Cells were lysed in RIPA buffer (50mM Tris-HCl, pH7.4, 150mM NaCl, 0.25% deoxycholic acid, 1% NP-40, 1mM EDTA). Protein concentrations were quantified with the Pierce BCA Protein Assay Kit (Thermo Fisher Scientific). For Western blotting, equal amounts of protein were heat denatured in the presence of a reducing agent and separated on 4-12% Bis Tris NuPage gels or 3-8% Tris-Acetate NuPage gels (Thermo Fisher Scientific), and transferred to PVDF membranes. Antibodies used for Western blotting were as follows: BRD7 (Cell Signaling, clone D9K2T), PBRM1 (Cell Signaling, clone D3F70), ARID2 (Abcam, ab51019) and GAPDH (Cell Signaling, clone D16H11), OTULIN (Cell Signaling, #14127), DUSP6 (Abcam, #ab76310) and NF1 (Cell Signaling, #14623). Proteins were detected using ECL Plus (GE Healthcare Life Sciences) using the ChemiDoc Imaging System (Bio-Rad). For total protein measurement, whole cell lysates were loaded to TGX Stain-Free gel (BIO-RAD) and ChemiDoc Imaging System (Bio-Rad) was used for image acquisition.

In vivo experiments with *Pbrm1*-deficient B16F10 cells

$2.5x10^5$ control (non-targeting gRNA) or *Pbrm1*-deficient B16F10-Cas9 cells were subcutaneously injected into 7 to 8 week old male C57BL/6 mice (The Jackson Laboratory, #000664). Three treatment groups were compared for mice implanted with control or *Pbrm1*-deficient B16F10 tumor cells: CD8 depletion (n=5-8 mice/group), αCTLA-4 plus αPD-1 (n=10 mice/group) and isotype control antibody (n=5-7 mice/group). In the CD8 depletion groups, CD8β mAb (clone53-5.8, #BE0223, 100μg/mouse) was administered on day-1, day 0 and then every 4th day. For the checkpoint blockade treatment groups, αPD-1 (clone 29F.1A12, #BE0273, 200μg/mouse) plus αCTLA-4 (clone 9H10, #BP0131, 100μg/mouse) mAbs were administered on day 4 and then every 3rd day. In the control groups, isotype control antibodies (2A3 and polyclonal syrian hamster IgG, 200μg/mouse and 100μg/mouse, respectively) were administered starting on day 4, and then every 3rd day. When tumors became palpable, their size was recorded with digital calipers every 2-3 days. Mice were sacrificed when tumors reached 20mm in diameter. All experiments were performed in compliance with federal laws and institutional guidelines and were approved by the Animal Care and Use Committee of the Dana-Farber Cancer Institute.

FACS analysis with tumor infiltrating T cells

$5x10^5$ control (non-targeting gRNA) or *Pbrm1*-deficient B16F10-Cas9 cells were subcutaneously injected into 7 to 8 week old male C57BL/6 mice. Mice were administrated with

checkpoint blockade antibodies (αCTLA-4 plus αPD-1) starting from day 3 and then every third day. Tumors were harvested on day 15, and single cell suspensions were stained with the following antibodies: anti-CD3 (17A2, BV510), anti-CD4 (RM4-5, BV785), anti-CD8 (53-6.7, BV650), anti-CD45 (30-F11, APC), anti-B220 (RA3-6B2, FITC), anti-NK1.1 (PK136, FITC) (Biolegend), anti-CD19 (MB19-1, FITC), anti-granzyme B (NGZB, PE-Cy7) (Thermo Fisher Scientific) and with fixable Zombie UV viability dye (Biolegend). BD LSRFortessa X-20 was used for data acquisition and FlowJo (Tree Star) was used for data analysis.

Analysis of MHC class I and PD-L1 expression by flow cytometry

Control (non-targeting gRNA), *Arid2*, *Pbrm1* and *Brd*7-deficient B16F10 cells were treated with different doses (0, 0.1, 0.5, 1, 5 or 10ng/ml) of IFNγ for 24 hours in triplicates. Cells were then stained with anti-H2-K^b (AF6-88.5, APC, Biolegend) or anti-PD-L1 (10F.9G2, APC, Biolegend) antibodies followed by FACS analysis. BD LSRFortessa X-20 was used for data acquisition and FlowJo (Tree Star) was used for data analysis. Geometric mean fluorescence intensity (gMFI) was calculated using FlowJo.

RNA-seq analysis

Total RNA was extracted from control (non-targeting gRNA), *Arid2*, *Pbrm1* and *Brd*7-deficient B16F10 cells cultured in complete DMEM in triplicates. Cells were stimulated with IFNγ (10ng/ml) or vehicle control for 24 hours. RNA extraction was performed using the RNeasy Plus Mini Kit (Qiagen, # 74134) following the manufacturer's protocol. Total RNA was submitted to the Molecular Biology Core Facility at DFCI for sequencing. Standard mRNA library preparation kit (RS-122-2101, Illumina) was used for library preparation. Single-end 75bp sequencing was done on Illumina NextSeq 500. Statistics for differentially expressed genes were calculated by DESeq2 (version 3.5)(*41*) and Cufflinks(*42*).

ATAC-seq

Control (non-targeting gRNA) and *Pbrm1*-deficient B16F10 cells were cultured in complete DMEM media in 10cm dishes. Cells were treated with 10ng/ml IFNγ or vehicle control for 24 hours. ATAC-seq was performed on triplicates (200,000 cells) by the Center for Functional Cancer Epigenetics at DFCI as previously described (*43, 44*). For data analysis, we used Burrows-Wheeler Aligner (BWA) (*45*) to map sequencing reads to the reference genome and MACS2 (*46*) for peak calling. DESeq2 (*41*) was applied to identify the differentially accessible regions with or without IFNγ treatment from ATAC-seq data. Binding and expression target analysis (BETA) (*47*) was used to integrate ATAC-seq data on accessible chromatin sites with differential gene expression data to infer directly targeted genes.

Gene sets enrichment analysis (GSEA)

For gene set identification, the hypergeometric overlap statistic tool (http://software.broadinstitute.org/gsea/msigdb/annotate.jsp) was used to calculate the overlap between a gene list and pathways in MSIgDB (Molecular signature database) (*48, 49*). GSEA on gene expression data was performed by loading cufflink count table for each comparison into the GSEA package.

Single-cell RNA-seq

$5x10^5$ control (non-targeting gRNA) or *Pbrm1*-deficient B16F10-Cas9 cells were subcutaneously injected into 7 to 8 week old male C57BL/6 mice (n=5 for each group). Mice were administrated with checkpoint blockade antibodies (αCTLA-4 plus αPD-1) starting from day 3 and then every third day. On day 15, tumors were harvested and 9,000 CD45+ live (DAPI negative) cells were sorted from each individual tumor by BD FACS Aria II. Sorted CD45+ cells were then combined for each group (total ~45,000 CD45+ cells for each genotype) and washed with 0.04% RNase-free BSA (Thermo Fisher Scientific) in PBS. 5,000 cells per condition were targeted for the 10X Genomics 3' single cell assay (10X Genomics). Reverse transcription, cDNA amplification and library preparation were performed according to manufacturer's protocols. Completed libraries were sequenced on an Illumina HiSeq 2500 on rapid-run mode, yielding >40,000 reads per cell.

Single-cell RNA-seq data analysis was performed using the Cell Ranger Single-Cell Software Suite provided by 10X Genomics: https://support.10xgenomics.com/single-cell-gene-expression/software/downloads/latest. Briefly, UMI counts were obtained by sequence alignment followed by barcode demultiplexing. The gene expression matrix was filtered to include only genes with at least one UMI count in at least one cell. Raw UMI counts were normalized by the total counts in each cell. The 1,000 genes with highest dispersion values (defined as the variance divided by the mean) were selected for further analysis. The UMI counts were log-transformed and z-score normalized for each gene. tSNE analysis was carried out based on the first 50 principal components obtained from PCA analysis. Distinct cell subpopulations were identified using k-means clustering. Differential expression analyses were performed by using the zlm.SingleCellAssay function in the R MAST package with method "glm". Hypergeometric overlap statistic tool (http://software.broadinstitute.org/gsea/msigdb/annotate.jsp) was used for GSEA analysis for single cell data.

ELISA

Cells ($1X10^6$) were plated in 6-well plates with complete growth medium. On the following day, cells were washed with serum-free medium three times and treated with IFNγ at indicated concentrations for 24 hrs. Chemokines were measured in supernatants using mouse CXCL9 (MIG) ELISA Kit and mouse CRG-2 (CXCL10) ELISA Kit (Thermo Fisher Scientific) according to the manufacturer's protocol.

Quantitative real-time PCR

Cells were treated with indicated concentrations of IFNγ for 24 hours and total RNA was isolated by RNeasy Plus Mini Kit (Qiagen). cDNAs were synthesized from 1 μg of total RNA using the PrimeScript RT reagent Kit (Takara) and were amplified by SYBR Premix Ex Taq II (Takara) using CFX96 Real-Time PCR System (Bio-Rad) according to the manufacturer's protocols. Primers for Cxcl9 and Gapdh were as follows: Cxcl9; 5'-AGTCCGCTGTTCTTTTCCTC-3' and 5'-TGAGGTCTTTGAGGGATTTGTAG-3', Gapdh; 5'-GTGTTCCTACCCCCAATGTGT-3'and 5'-ATTGTCATACCAGGAAATGAGCTT-3'. Relative mRNA expression was evaluated after normalization for Gapdh expression.

Growth competition assay

PBAF mutant (GFP+) and control B16F10-Cas9 cells (GFP-) were mixed at 1:1 ratio. The mixture of cells was then seeded in 10cm dish in complete growth medium. Cells were passaged every three or four days and were analyzed by flow cytometry for changes of the ratio of GFP+/GFP- cells.

Doxorubicin-induced cell death

Two knockout B16F10 cell lines with independent gRNAs were generated for *Otulin*, *Dusp6* and *Nf1* using the same protocol as described for PBAF complex. The knockout cell lines (GFP+) were mixed with control cells (GFP-) at 1:1 ratio. The mixture of cells was then seeded at 200,000 cells/well in a 6-well plate. Eighteen hours after seeding, different doses of doxorubicin (Sigma-Aldrich, D1515) as indicated in Fig. S5 were added to the cell culture (triplicate wells / condition). After 24 or 48 hours, cells were harvested and stained with DAPI (5μg/ml) for 5 minutes in PBS with 2% FBS at room temperature. The ratio of GFP+/GFP- was determined by FACS (gated on DAPI- for live cells).

Supplementary Figures

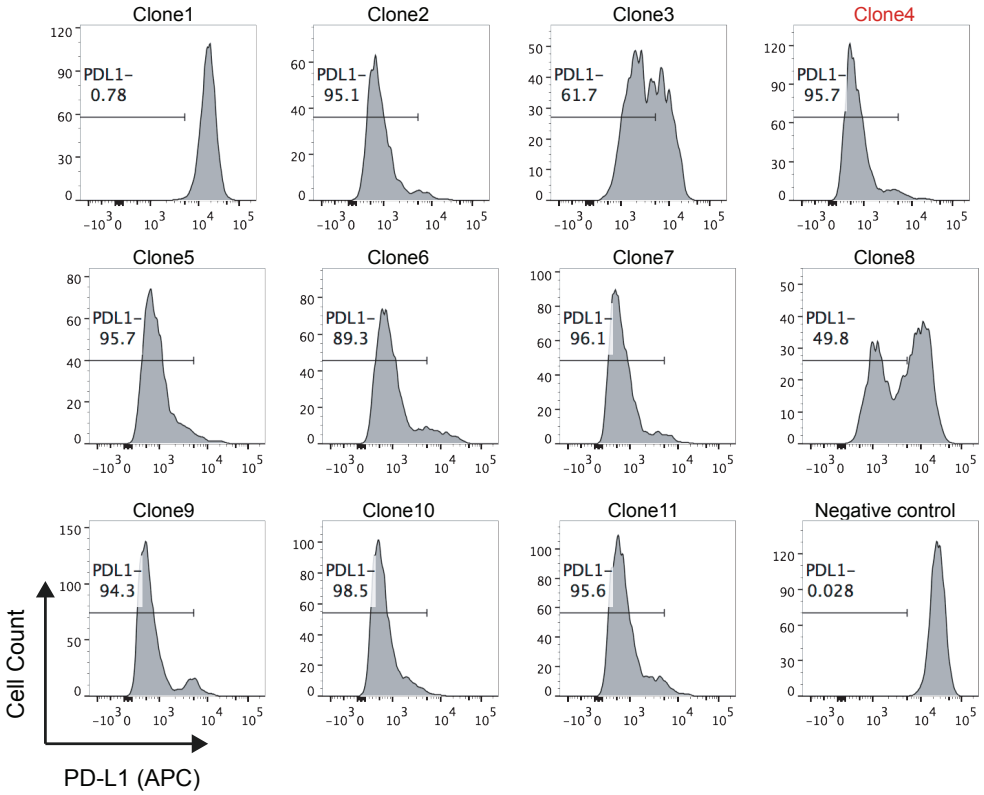

Fig. S1. Selection of B16F10 clones with high Cas9 editing activity.

B16F10 cells were transduced with a lentiviral vector driving Cas9 expression and individual cells were sorted into 96 well plates based on co-expression of a GFP marker. Each B16F10 clone was independently transduced with a lentivirus encoding a gRNA targeting PD-L1. Ten days post transduction, Cas9 editing efficiency was determined based on the percentage of PD-L1 negative cells following treatment with IFNγ (10ng/ml) for 24 hours. Clone4 which had an editing efficiency >95% was selected for the screen to enable sensitive detection of depleted gRNAs in the screen. High editing efficiency is important in such a screen because non-edited tumor cells would mask detection of depleted gRNAs.

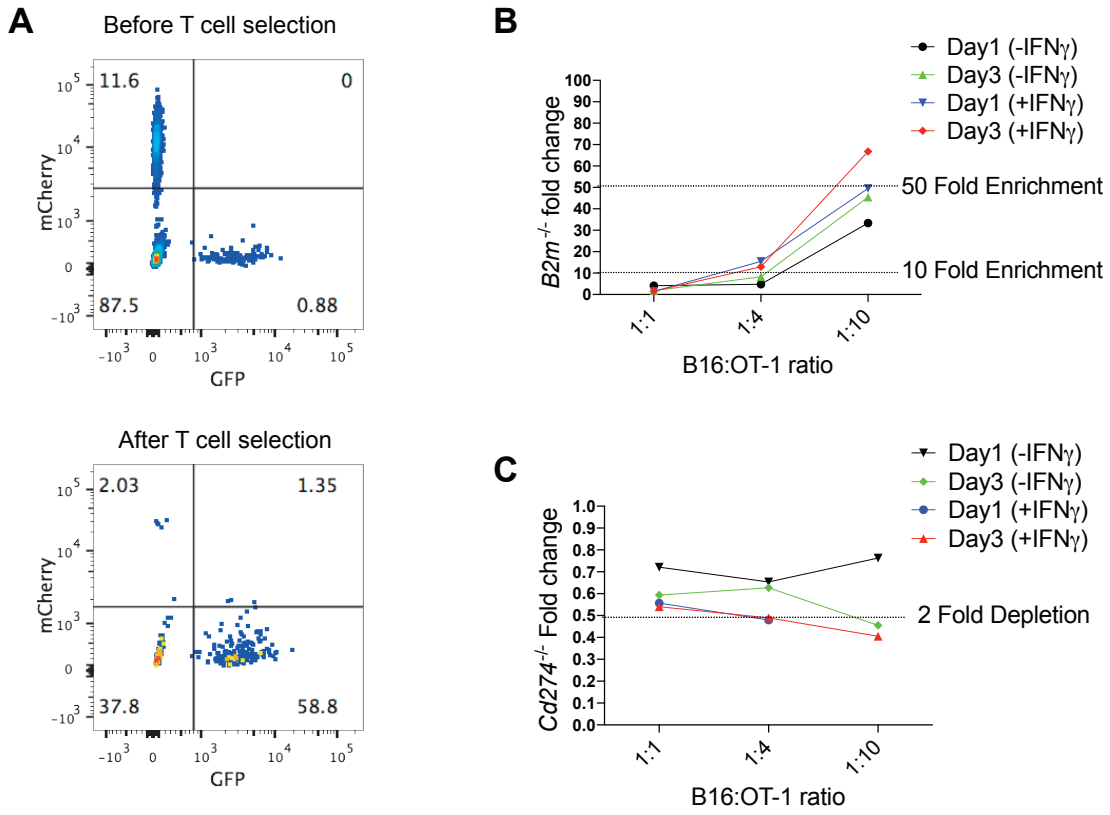

Fig. S2. Positive controls for discovery of positive and negative immune regulators expressed by tumor cells.

(**A**) B2m-deficient (GFP+) and Cd274 (PD-L1)-deficient (mCherry+) B16F10 cells were mixed with unmodified B16F10 cells (targeting a composition of ~1% GFP+ and 10% mCherry+ cells prior to co-culture with T cells). Tumor cells were pulsed with 1ng/ml of SIINFEKL peptide for two hours. These tumor cell populations were then co-cultured with OT-I T cells at different tumor to T cell ratios for one day or three days. Representative FACS plots of B16F10 cell populations before and after co-culture with T cells. (**B-C**) Summary of results (fold change) for B2m-/- (top) and Cd274-/- (bottom) B16F10 tumor cells following selection by OT-1 T cells depending on the following experimental variables: (1) B16F10 tumor to OT-I T cell ratio, (2) time period of co-culture, and (3) pretreatment of B16F10 cells with or without IFNγ (10 ng/ml) prior to co-culture with T cells to increase H2-K^b expression by tumor cells. Data are representative of at least two independent experiments.

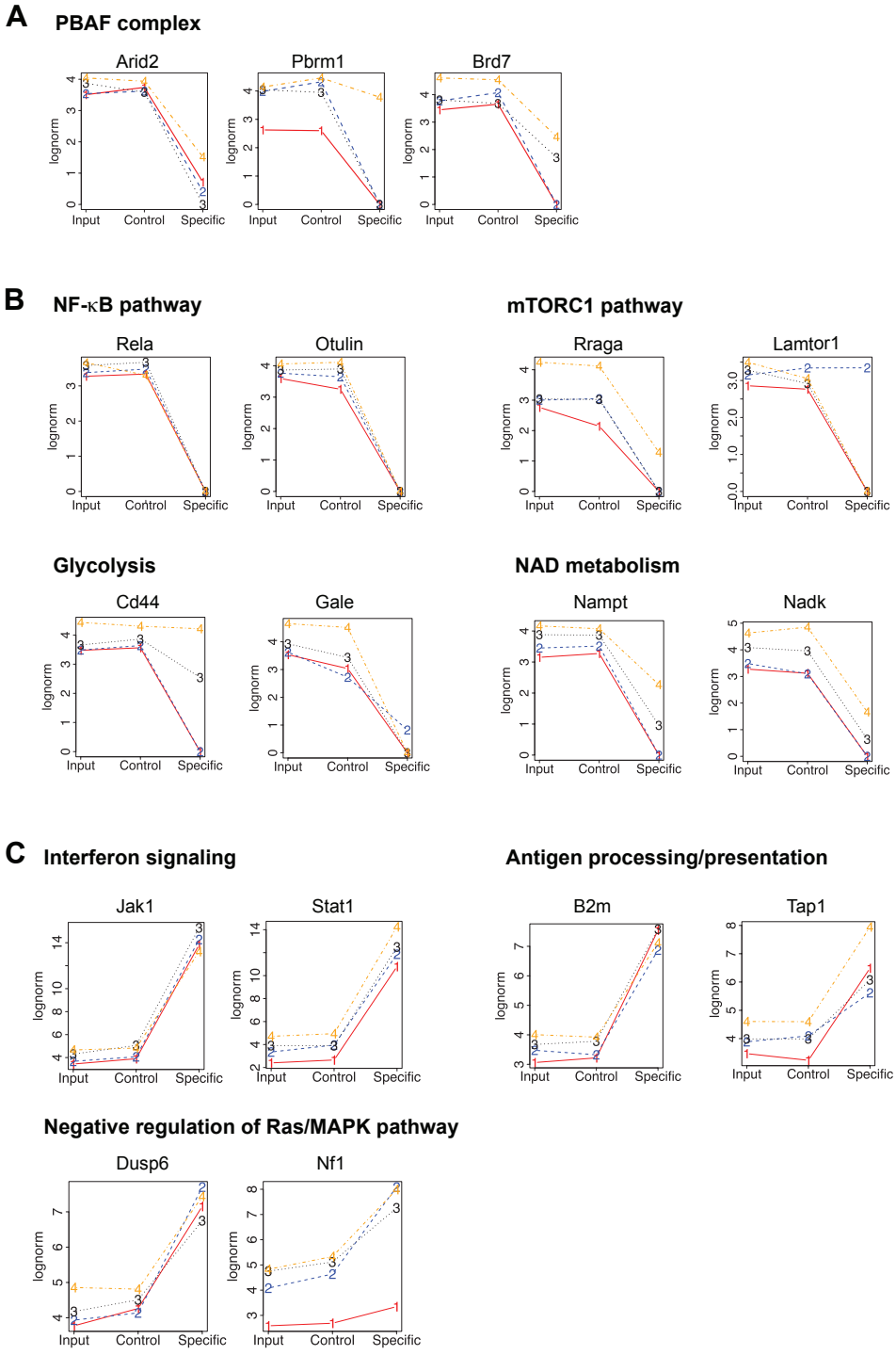
A
PBAF complex
Arid2
Pbrm1
Brd7
B
NF-κB pathway
Rela
Otulin
mTORC1 pathway
Rraga
Lamtor1
Glycolysis
Cd44
Gale
NAD metabolism
Nampt
Nadk
C
Interferon signaling
Jak1
Stat1
Antigen processing/presentation
B2m
Tap1
Negative regulation of Ras/MAPK pathway
Dusp6
Nf1
lognorm
Input
Control
Specific

Fig. S3. Analysis of gRNA representation in experimental and control screening conditions.
gRNA frequencies were analyzed for key genes identified in the screen for which gRNAs were either depleted (**A, B**) or enriched (**C**) in the presence of tumor-specific cytotoxic T cells. These genes included all three unique members of the PBAF complex (*Pbrm1*, *Arid2* and *Brd7*) (**A**), and two representative members of major pathways presented in Fig.1D (**B, C**). For each gene, the frequencies of all four gRNAs in the primary screen were plotted for three conditions: Input tumor library (Input), control selection with T cells of irrelevant TCR specificity (Control) and experimental selection with tumor-specific Pmel-1 T cells (Specific); y-axis: Log normalized count for each condition.

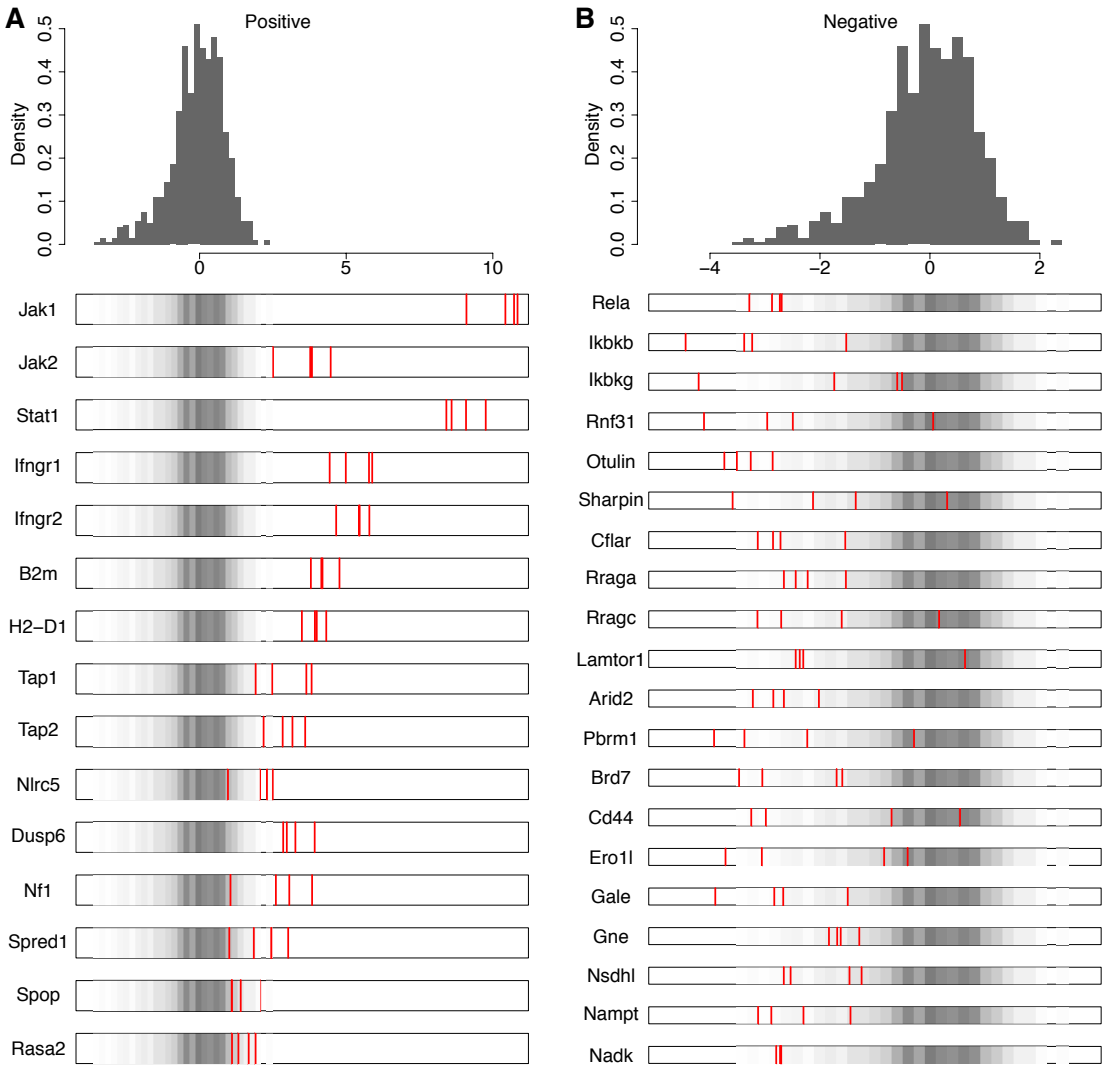

Fig. S4 Frequency histograms of enriched and depleted gRNAs.

In Pmel1 primary screen, Log2 fold change of enriched **(A)** or depleted **(B)** gRNAs for each gene presented in Figure 1D are labelled with red lines. Distribution of 1,000 non-targeting control gRNAs is also indicated in both histograms (grey scale).

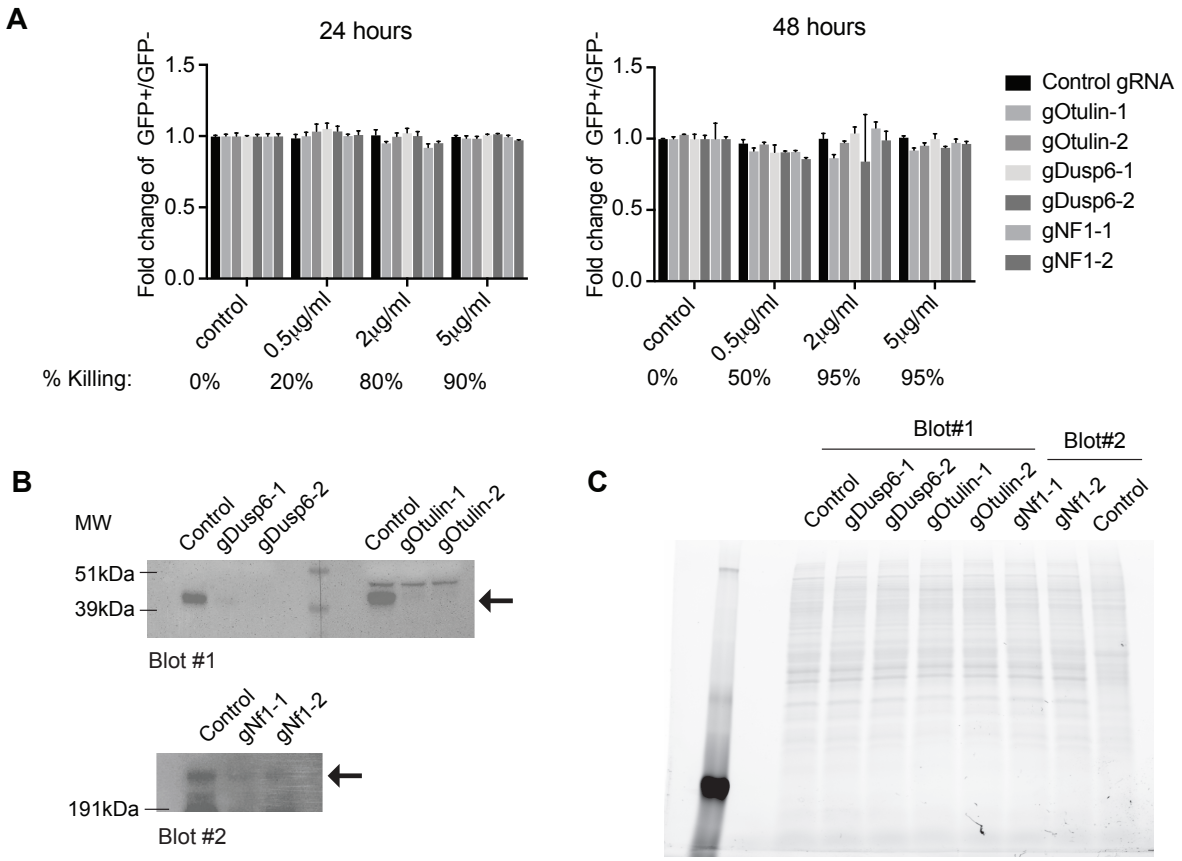

Fig. S5. Testing of the cell death threshold for *Otulin*, *Dups6* and *Nf1*-deficient B16F10 cells.

(A) *Otulin*, *Dusp6* and *Nf1*-deficient B16F10 cells (two gRNAs for each gene) were evaluated for their sensitivity to doxorubicin induced cell death. GFP expressing *Otulin*, *Dusp6* and *Nf1*-deficient B16F10 cells were mixed with GFP-negative control B16 cells at a 1:1 ratio. Cells were treated with different concentrations of doxorubicin or vehicle control for 24 (left) or 48 (right) hours. Fold change of the percentage of GFP+ cells following doxorubicin treatment was measured by FACS. The total % killing of tumor cells in response to doxorubicin is indicated below the graphs. **(B)** Western blot showing protein levels of Dusp6, Otulin and Nf1 in control and indicated knockout cell lines. **(C)** The same cell lysates as in (B) were loaded on a TGX stain-free gel (Bio-Rad) to assess the amount of total protein in each sample. Data shown in (A) are representative of two independent experiments.

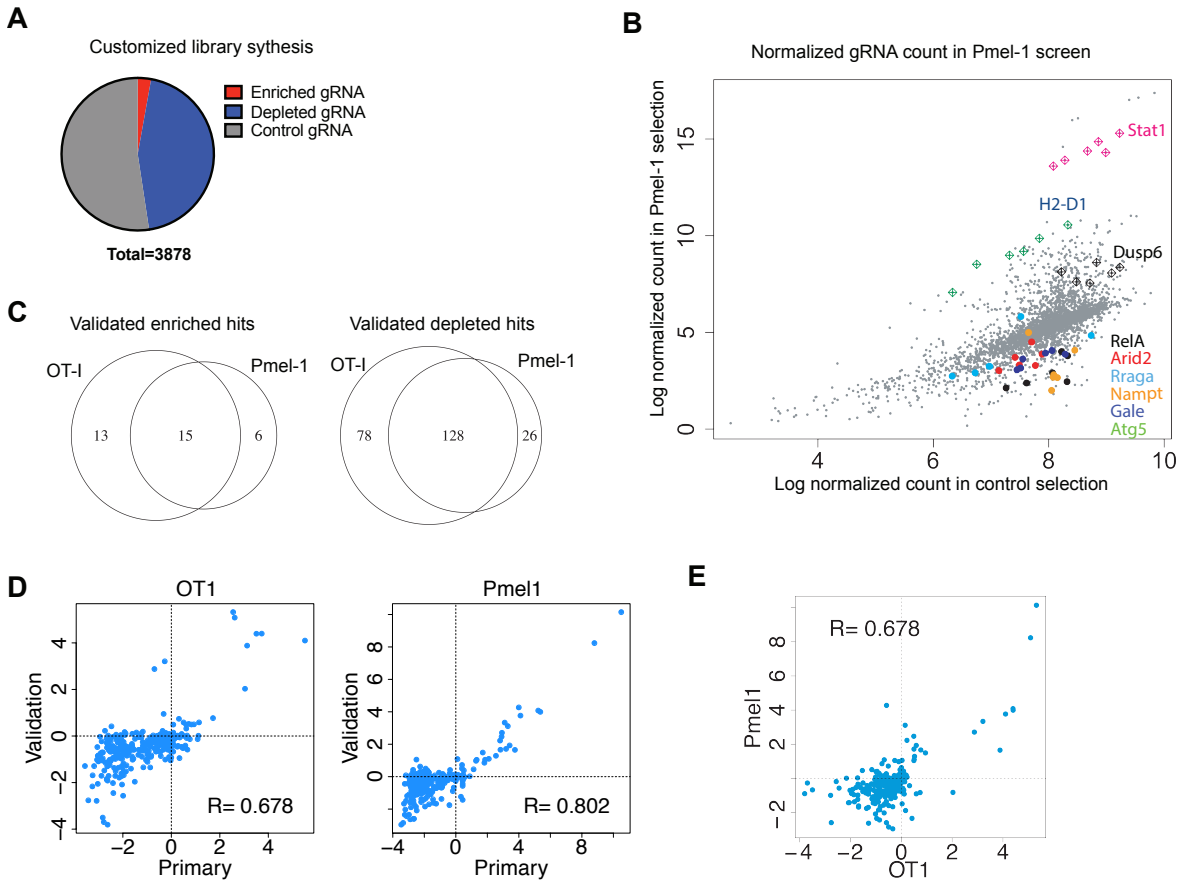

Fig. S6. Validation of candidate genes by screening of a mini-pool gRNA library.

(**A**) Mini-pool library design. The most significant hits (LFC>2 and FDR<0.05) from Pmel-1 and OT-I screens (total of 313 genes) were included in the mini-pool gRNA library. The library contained 6 gRNAs for each candidate gene (total 1,878 targeting gRNAs) and 2,000 non-targeting control gRNAs. **(B)** Normalized counts for each gRNA with Pmel-1 selection (Y-axis) or control T cell selection (X-axis). Examples of enriched and depleted gRNAs were annotated. (**C**) Summary of validation screen. Venn diagram illustrating validated genes for enriched gRNAs (n=15 genes) and depleted gRNAs (n=128 genes) that were positive in both Pmel-1 and OT-I screens (FDR<0.05 in MaGeCK analysis). (**D**) The correlation between different screening results. The log-fold change (logFC) ratios of primary screens are plotted on the X-axis, while the logFC of the validation screen is on the Y-axis. The OT1 and Pmel-1 conditions are shown separately. (**E**) The correlation between OT-I and Pmel1 validation screens. The log-fold change (logFC) ratios of OT1 screens are plotted on the X-axis, with the Pmel1 screen logFC on the Y-axis.

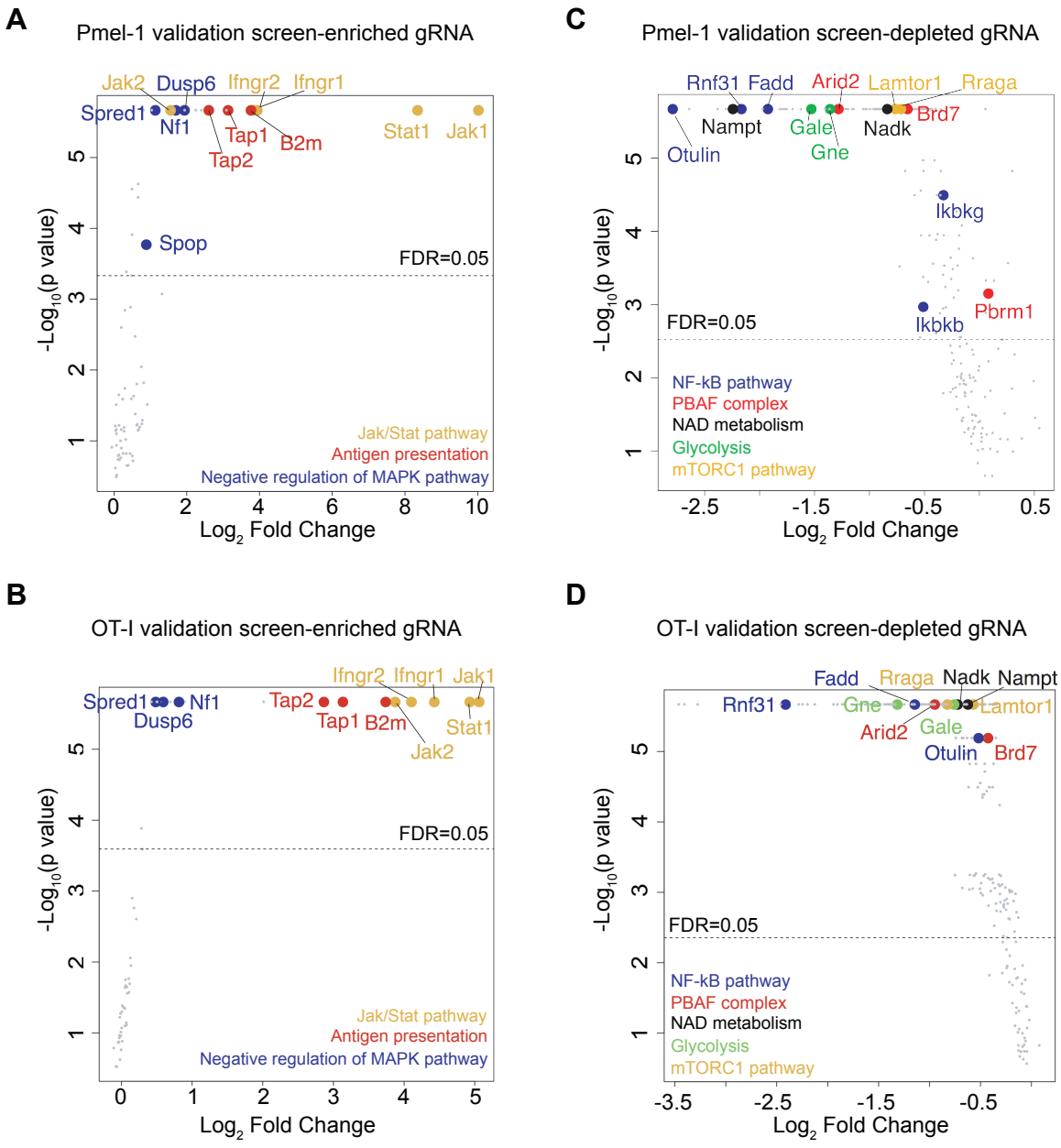

Fig. S7. Genes validated in screens with Pmel-1 and OT-I T cells.

(**A, B**) Validation data for genes with enriched gRNAs in screens with Pmel-1 (A) and OT-I (B) T cells analyzed using MaGeCK software. Candidate genes were plotted based on mean log2 fold change of gRNA counts and p values. Genes involved in MHC/antigen presentation pathway (red), type I/II interferon pathways (yellow) and Ras/MAPK pathway (blue) were annotated. (**C, D**) Validation data for top genes with depleted gRNAs in screens with Pmel-1 (C) and OT-I (D) T cells. Selected genes involved in NF-kB (blue), mTORC1 pathway (yellow),

PBAF form of SWI/SNF complex (red), NAD metabolism (black), and glycolysis (green) were highlighted.

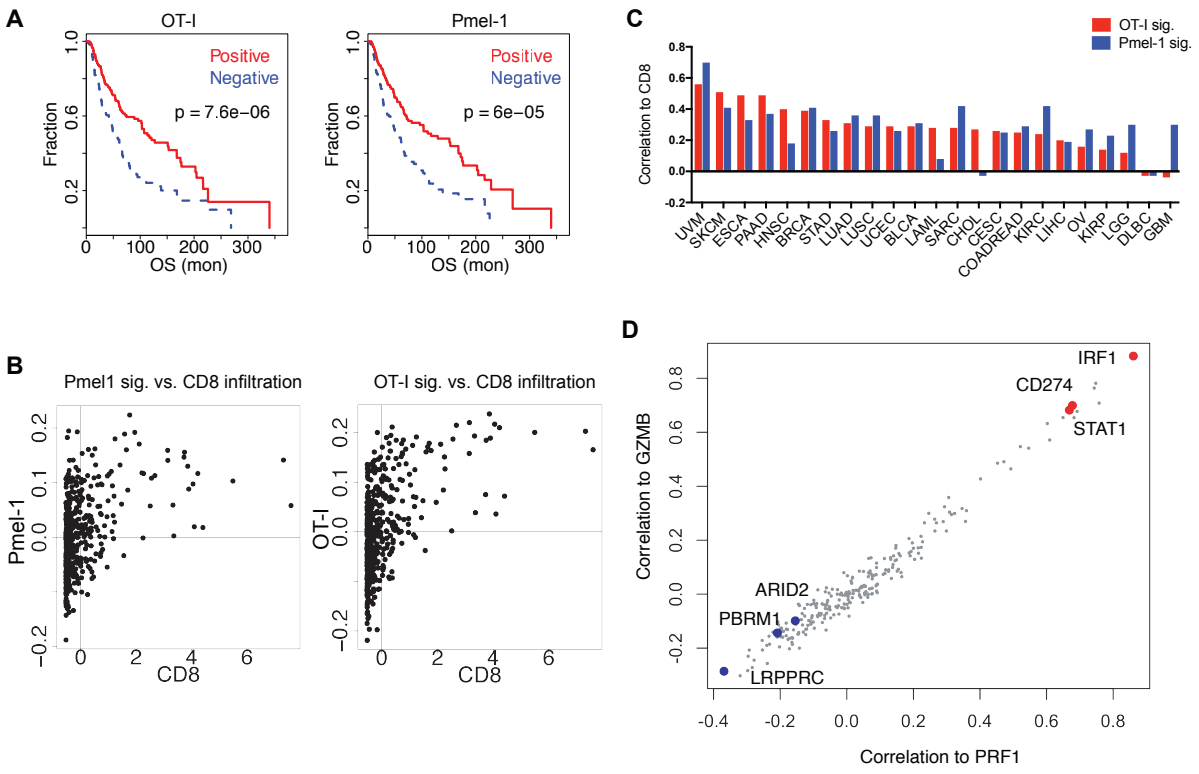

Fig. S8. Correlation of discovered genes in TCGA datasets of human cancer.

(A-C) OT-I and Pmel-1 gene sets were associated with improved survival and increased CD8 T cell infiltration in TCGA melanoma patients. (**A**) Impact of discovered gene sets on survival of melanoma patients. For each patient in the TCGA melanoma study, the Pearson correlation value was computed between gene expression values in melanomas for all genes identified in the OT-I or Pmel-1 screens and log2 fold enrichment/depletion of gRNAs for genes identified in CRISPR/Cas9 screen. The overall survival (OS) durations are shown for patients with positive and negative correlations. Comparison of survival between groups was analyzed through two-sided Ward test in CoxPH. (**B**) Correlation of CRISPR screening data with estimated CD8 T cell infiltration in TCGA melanoma data. For each patient in TCGA melanoma study, the average value of CD8A+CD8B mRNA level (X-axis, marker of CD8 T cell infiltration) was plotted against correlation value (Y-axis) determined in (A) for CRISPR screening data (log2 fold ratios). (**C**) For each patient in TCGA, we computed a correlation signature between gene expression profile and log2 fold change of top CRISPR gene hits. This patient signature was related to average value of CD8A+CD8B mRNA level across patients in each cancer type through Pearson correlation. (**D**) For each of the top hits identified in the screen, Spearman's correlation of its expression level to GZMB or PRF1 expression level in TCGA melanoma patients were computed and plotted. Examples with positive (red) and negative (blue) correlations were annotated.

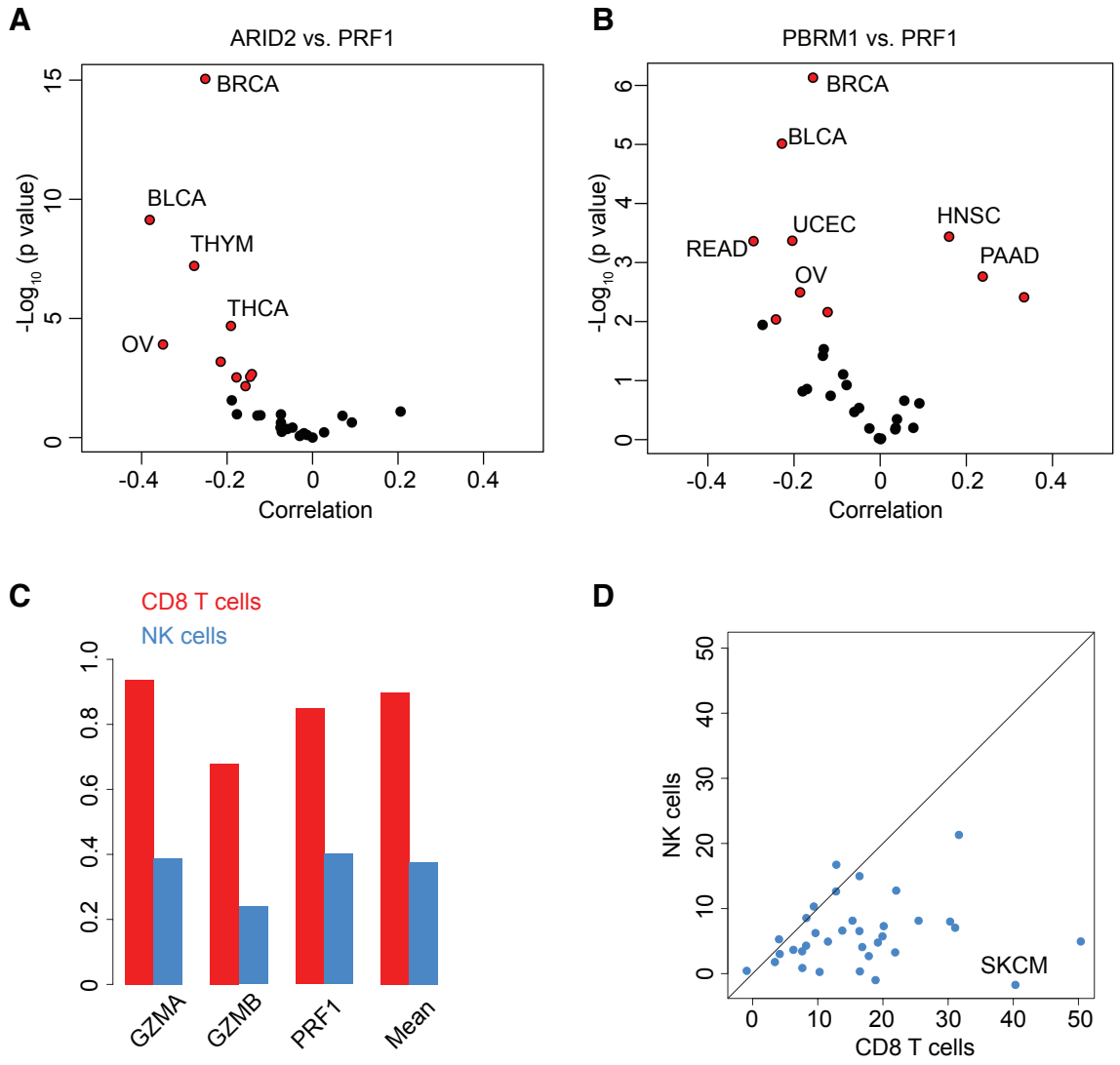

Fig. S9. Correlation of ARID2 and PBRM1 expression to T cell cytotoxic markers in TCGA data.

(**A, B**) Volcano plots showing the Spearman's correlation and estimated significance (log10 p-value) of ARID2 (**A**) or PBRM1 (**B**) expression with PRF1 (perforin) expression across all TCGA cancer types using Tumor Immune Estimation Resource (TIMER) (tumor purity adjusted) (*32*). Each dot represents a cancer type in TCGA, with red dots indicating a significant correlation ($p<0.01$). **(C, D)** Relative contribution of CD8 T cells and NK cells to the immune-mediated cytotoxicity. (**C**) Correlation between the estimated CD8 T cell or NK cell infiltration and immune cytotoxicity markers. (**D**) Comparison of relative contribution to immune cytotoxicity between CD8 T and NK cells, with the line of equal contribution on the diagonal. In each cancer type, the CD8 T cell level was estimated through the expression sum of CD8A and CD8B. The NK cell level was estimated through expression of NCR1 (NKp46). Immune cytotoxicity was estimated through expression sum of GZMA, GZMB and PRF1. In each cancer,

a linear regression was fitted with CD8 T, NK cell levels as the covariates and immune cytotoxicity as the outcome. The t-values of T cells and NK cells, representing their relative contribution to the immune cytotoxicity, were plotted across all TCGA cancer types. This analysis indicates that cytotoxicity markers are more closely associated with estimated T cell than NK cell infiltration.

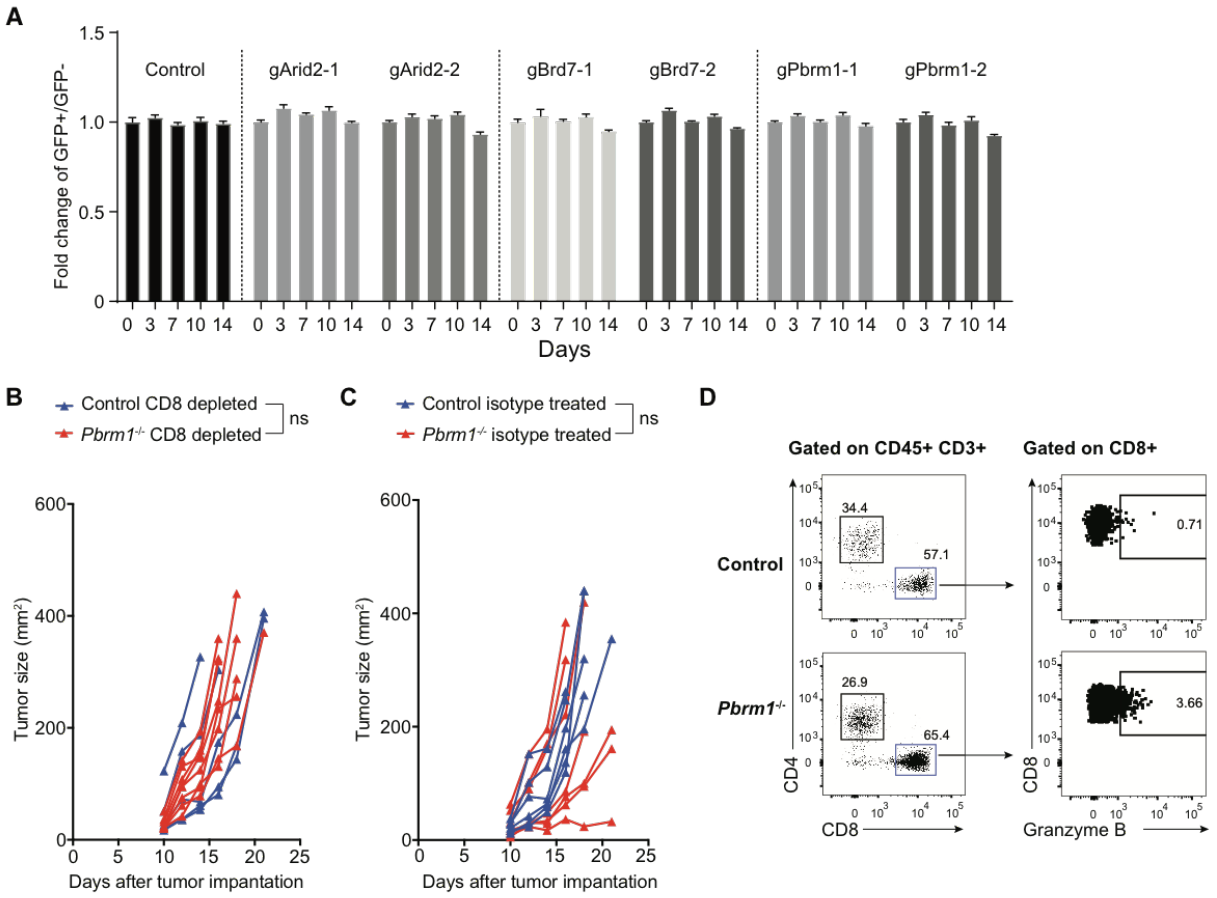

Fig. S10. Characterization of *Pbrm1*-deficient B16F10 tumor cells *in vitro* and *in vivo*.

(A) GFP-expressing *Arid2*, *Pbrm1* or *Brd7*-deficient B16F10 cells were mixed with GFP-negative control B16F10 cells at a 1:1 ratio and grown *in vitro* for 2 weeks. The ratio of GFP-positive vs. GFP-negative cells was assessed at different time points to determine if inactivation of the PBAF complex had an impact on tumor cell growth or survival *in vitro*. Values represents mean +/- SD. (**B-C**) Related to Fig.3D, mice bearing control or *Pbrm1*-deficient B16F10 tumors (n=5-8) were treated with CD8 depleting mAb (**B**) or isotype control antibody (2A3 and polyclonal Syrian hamster IgG) (**C**), and tumor size was measured. Two-way ANOVA was used to determine statistical significance for time points when all mice were viable for tumor measurement. ns, not significant. (**D**) Related to Fig. 3F, flow cytometric analysis of granzyme B expression by tumor-infiltrating CD8 T cells in *Pbrm1*-deficient and control B16F10 tumors. All data shown in this figure are representative of two independent experiments.

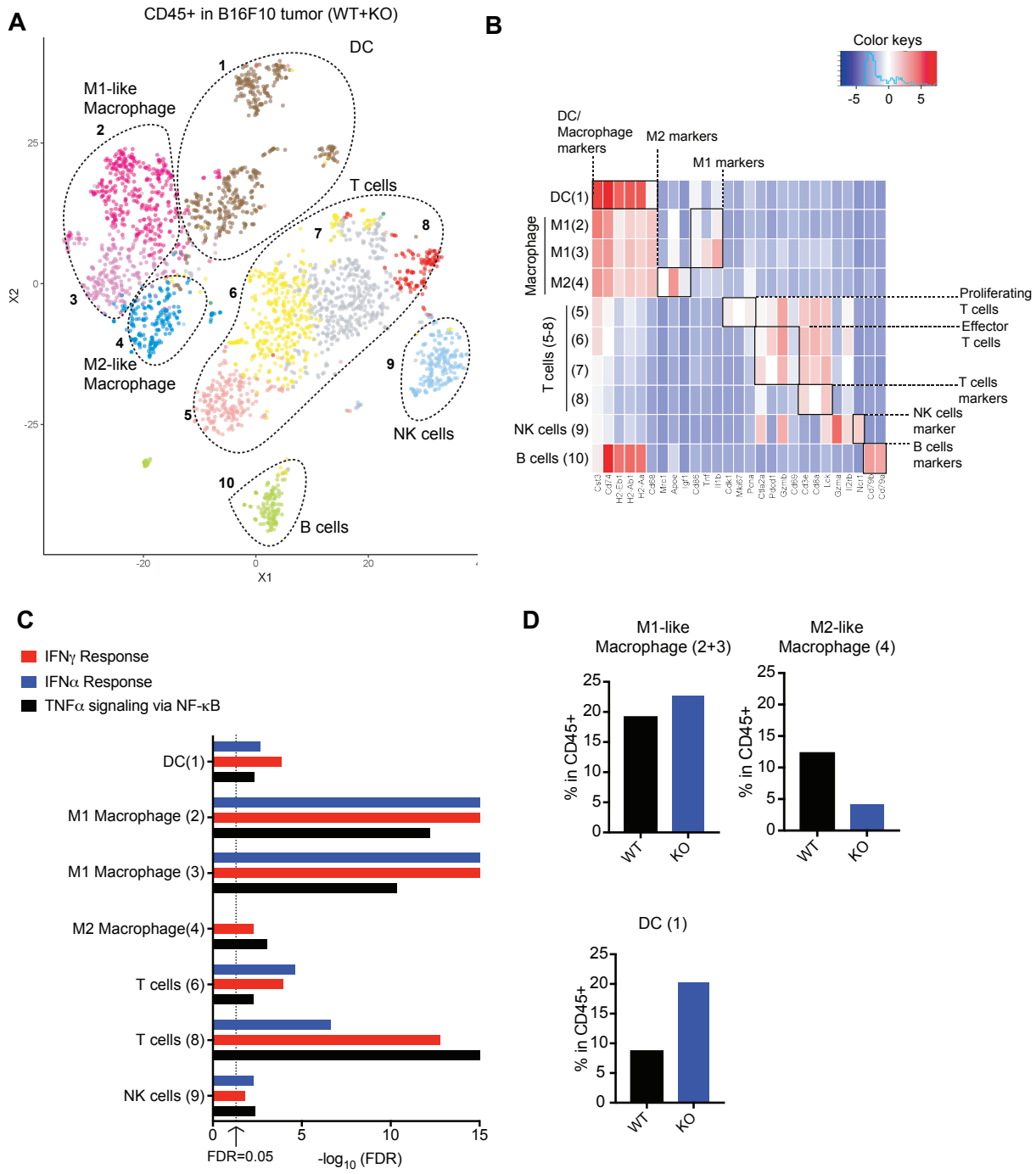

Fig. S11. Changes in tumor microenvironment in *Pbrm1*-deficient tumors.

(A) CD45+ cells were sorted and pooled (n=5) from either *Pbrm1*-deficient or control B16F10 tumors for single-cell RNA-seq. tSNE projections of CD45+ cells are shown (combined for *Pbrm1*-deficient and control B16F10 tumors). Cells are colored by k-means clusters, and the

corresponding cell types are annotated based on expression of lineage-specific markers as illustrated in (B). (**B**) Heatmap showing the gene expression level of markers for each cluster of cells separated by k-means clusters. (**C**) GSEA analysis (hallmark gene sets) was performed on genes that were significantly overexpressed in *Pbrm1*-deficient compared to control B16F10 tumors for each k-means cluster shown in (**A**); –log10 (FDR) for "IFNα response", "IFNγ response" and "TNFα signaling via NF-κB" gene sets are shown. (**D**) Percentage of indicated cell clusters in total CD45+ cells in *Pbrm1*-deficient versus control B16F10 tumors.

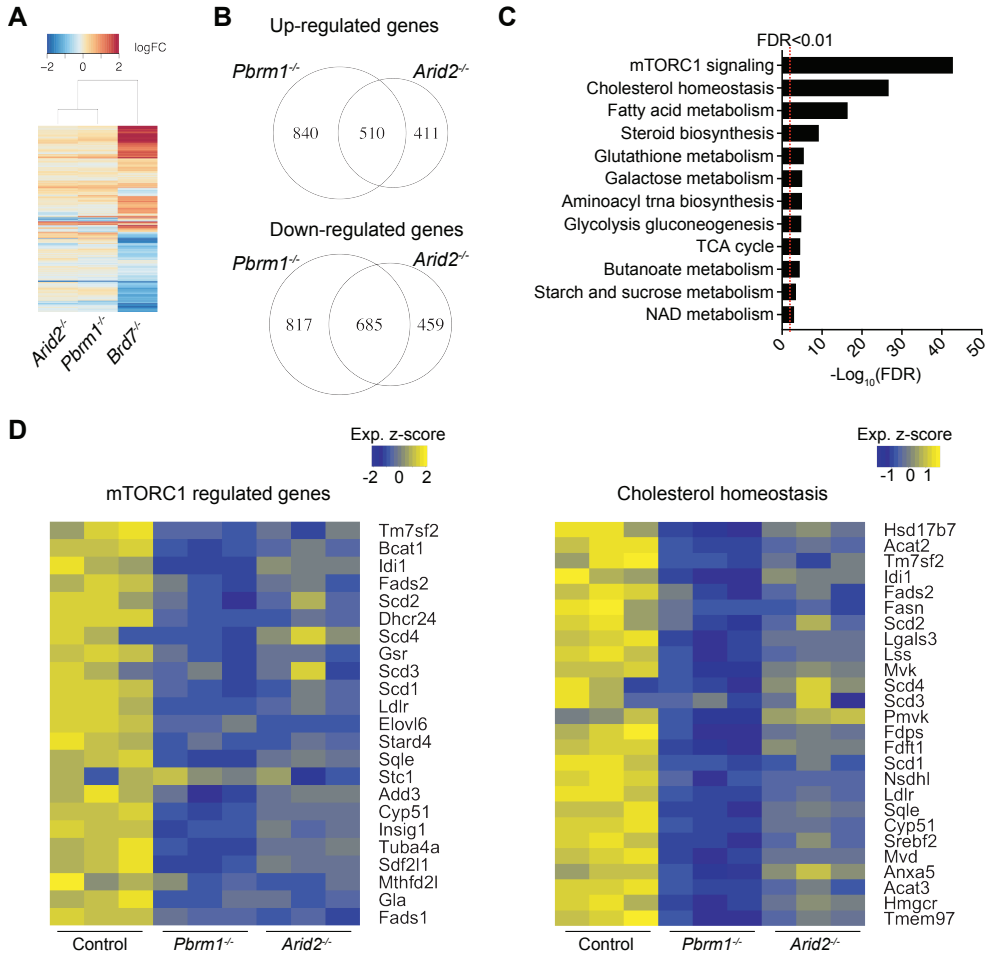

Fig. S12. Gene expression profiles of *Arid2*, *Pbrm1* and *Brd7*-deficient B16F10 tumor cells.
RNA-seq was performed on *Arid2, Brd7 or Pbrm1*-deficient cells as well as control B16F10 cells. (**A**) Heat map and clustering showing the overall log2 fold change in gene expression in *Arid2*, *Pbrm1* and *Brd7*-deficient B16F10 cells compared to control B16F10 cells (transduced with non-targeting gRNA). (**B**) Venn diagram showing the number of genes that were upregulated or downregulated in *Arid2* and/or *Pbrm1*-deficient B16F10 cells compared to control B16F10 cells in RNA-seq data. (**C**) Hypergeometric overlap statistics were used to test which Hallmark and KEGG gene sets were enriched among genes that were significantly downregulated in both *Arid2* and *Pbrm1*-deficient cells compared to control B16F10 cells. FDR q-values for top-ranked mTORC1 and several other metabolic genes sets are shown. (**D**) Heat map showing the expression value (z-score based on cufflink count) for genes in mTORC1 and cholesterol homeostasis gene sets for control, *Arid2* or *Pbrm1*-deficient B16F10 cells.

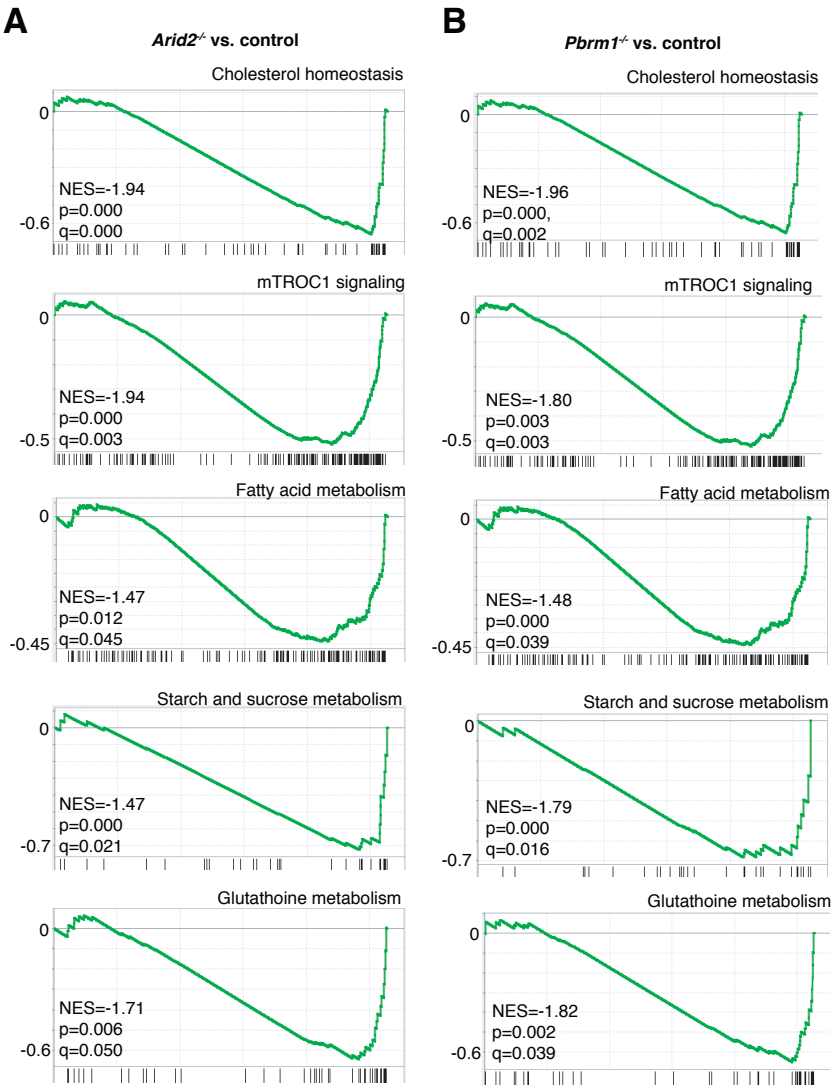

Fig. S13. GSEA analysis on *Arid2* and *Pbrm1*-deficient cells.

GSEA of differentially expressed genes (RNA-seq datasets) in *Arid2*-deficient cells versus control B16F10 cells (**A**) or *Pbrm1*-deficient cells versus control B16F10 cells (**B**). Gene sets for mTORC1 and several other metabolic pathways negatively enriched in *Arid2* and *Pbrm1*-deficient cells are shown.

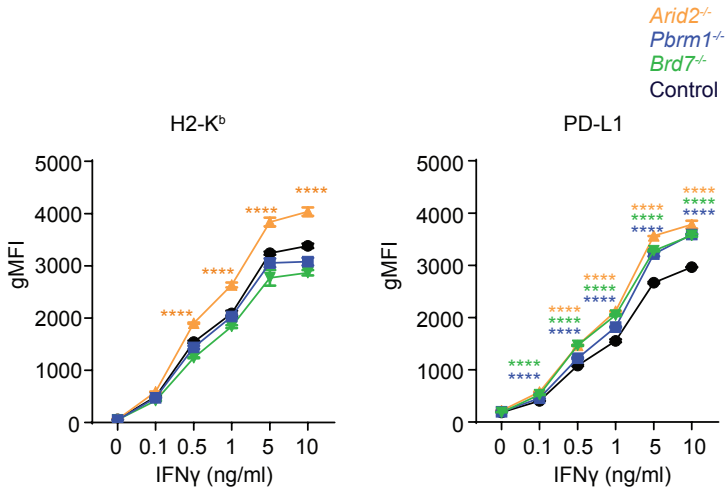

Fig. S14. The effect of PBAF complex on IFNγ induced expression of H2-K^b and PD-L1 induction.

Arid2, *Pbrm1* and *Brd7*-deficient cells and control B16F10 cells were treated with different doses of IFNγ and surface expression of H2-K^b and PD-L1 (geometric mean fluorescence intensity, gMFI) was determined by FACS after 24 hours. Two-way ANOVA was used to determine statistical significance (**** $p<0.0001$). Data shown are representative of two independent experiments.

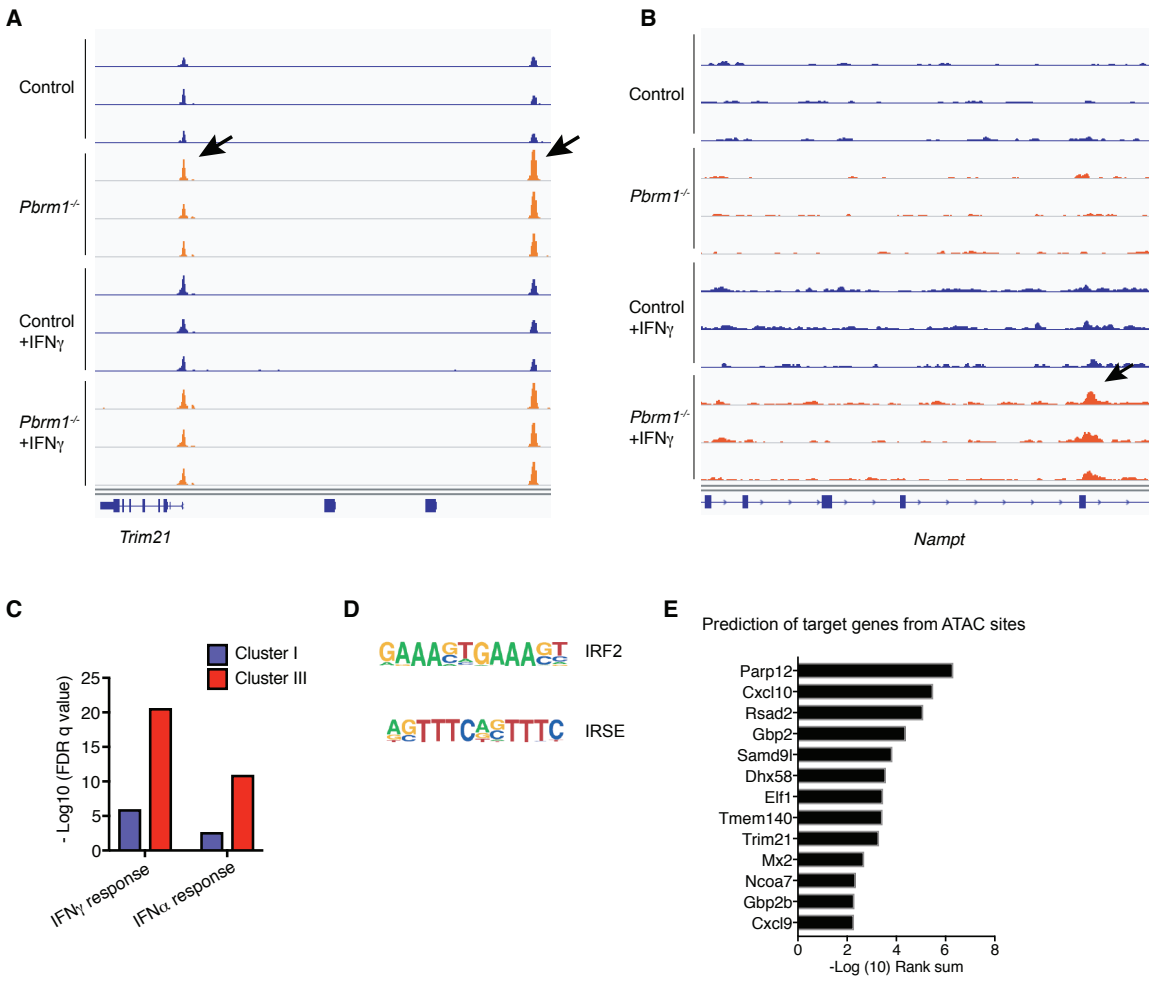

Figure S15. Analysis of chromatin accessibility in *Pbrm1*-deficient and control cells.

(**A**) Accessible sites near *Trim21* as example of interferon-responsive sites that were more accessible in *Pbrm1*-deficient cells prior to IFNγ stimulation (arrows). (**B**) Example of a cluster III site (as defined in Fig. 5B), which became more accessible in *Pbrm1*-deficient cells compared to control B16F10 cells following IFNγ treatment (arrow). (**C**) Hypergeometric overlap statistics were used to define Hallmark gene sets enriched in nearby genes for cluster I, II and III sites; IFNγ and IFNγ response gene sets are shown. (**D**) IRF2 and IRSE were the most significant motifs (computed by HOMER (*50*)) enriched in clusters I, II and III ($p<1e-37$). (**E**) Direct target prediction and statistical significance analysis was performed using BETA (Binding and Expression Target Analysis) based on ATAC-seq sites from clusters I and III and differentially expressed genes following IFNγ treatment in *Pbrm1*-deficient cells. Significant predicted targets for genes in Fig.4C are shown.

Table S1. Complete list of top candidate genes in Pmel-1 screen (FDR<0.05).

LogFC, Log(2) fold change; FDR, False Discovery rate. FDR and p value calculated by MaGeCK.

		Positive selection		Negative selection	
Gene	**logFC**	**p value**	**FDR**	**p value**	**FDR**
Jak1	9.69	2.39E-07	1.50E-04	1.00E+00	1.00E+00
Stat1	8.49	2.39E-07	1.50E-04	1.00E+00	1.00E+00
Ifngr2	4.87	2.39E-07	1.50E-04	1.00E+00	1.00E+00
Ifngr1	4.68	2.39E-07	1.50E-04	1.00E+00	1.00E+00
B2m	3.72	2.39E-07	1.50E-04	1.00E+00	1.00E+00
H2-D1	3.53	2.39E-07	1.50E-04	1.00E+00	1.00E+00
Jak2	3.10	2.39E-07	1.50E-04	1.00E+00	1.00E+00
Lztr1	2.91	2.39E-07	1.50E-04	1.00E+00	1.00E+00
Ube2g2	2.87	2.39E-07	1.50E-04	1.00E+00	1.00E+00
Dusp6	2.83	2.39E-07	1.50E-04	1.00E+00	1.00E+00
Tap1	2.55	2.39E-07	1.50E-04	1.00E+00	1.00E+00
Tap2	2.51	2.39E-07	1.50E-04	1.00E+00	1.00E+00
Derl2	2.39	2.39E-07	1.50E-04	1.00E+00	1.00E+00
Nf1	2.23	2.39E-07	1.50E-04	1.00E+00	1.00E+00
Syvn1	2.15	2.39E-07	1.50E-04	1.00E+00	1.00E+00
Mbnl1	2.15	2.39E-07	1.50E-04	1.00E+00	1.00E+00
Cic	1.94	2.39E-07	1.50E-04	1.00E+00	1.00E+00
Tbl1x	1.93	2.39E-07	1.50E-04	1.00E+00	1.00E+00
Aup1	1.93	2.39E-07	1.50E-04	1.00E+00	1.00E+00
Ube2j1	1.91	2.39E-07	1.50E-04	1.00E+00	1.00E+00
Ints10	1.91	2.39E-07	1.50E-04	1.00E+00	1.00E+00
Vgll4	1.65	2.39E-07	1.50E-04	1.00E+00	1.00E+00
Spred1	1.64	4.07E-06	1.91E-03	1.00E+00	1.00E+00
Fus	1.64	2.39E-07	1.50E-04	1.00E+00	1.00E+00
Cbx4	1.62	2.39E-07	1.50E-04	1.00E+00	1.00E+00
Pmel	1.53	2.39E-07	1.50E-04	1.00E+00	1.00E+00
Fbrs	1.51	2.39E-07	1.50E-04	1.00E+00	1.00E+00
Nlrc5	1.48	2.39E-07	1.50E-04	1.00E+00	1.00E+00
Sel1l	1.48	7.18E-07	4.24E-04	9.99E-01	1.00E+00
Xpnpep1	1.47	2.39E-07	1.50E-04	1.00E+00	1.00E+00
Mbnl2	1.46	2.16E-06	1.11E-03	1.00E+00	1.00E+00
Swi5	1.46	2.39E-07	1.50E-04	1.00E+00	1.00E+00
Asun	1.46	1.56E-05	6.57E-03	1.00E+00	1.00E+00
Usp24	1.45	1.20E-06	6.51E-04	1.00E+00	1.00E+00

Ifnar1	1.42	2.39E-07	1.50E-04	1.00E+00	1.00E+00
Cdkn1a	1.38	2.39E-07	1.50E-04	1.00E+00	1.00E+00
Ifnar2	1.37	7.18E-07	4.24E-04	1.00E+00	1.00E+00
Rfxank	1.37	2.42E-05	8.93E-03	1.00E+00	1.00E+00
Edem3	1.35	2.39E-07	1.50E-04	9.99E-01	1.00E+00
Nf2	1.33	3.59E-06	1.77E-03	1.00E+00	1.00E+00
Med13	1.29	2.39E-07	1.50E-04	1.00E+00	1.00E+00
Usp22	1.28	0.00010081	3.16E-02	1.00E+00	1.00E+00
Pvr	1.26	1.20E-06	6.51E-04	9.99E-01	1.00E+00
Ipo13	1.24	9.27E-05	2.95E-02	1.00E+00	1.00E+00
Kdm1a	1.20	4.07E-06	1.91E-03	9.99E-01	1.00E+00
Bbx	1.19	1.68E-06	8.89E-04	9.98E-01	1.00E+00
Chrac1	1.15	0.00016834	4.70E-02	1.00E+00	1.00E+00
Eloa	1.14	7.02E-05	2.34E-02	9.99E-01	1.00E+00
2310033P09Rik	1.08	2.08E-05	7.98E-03	9.99E-01	1.00E+00
Cdkn2c	1.08	2.75E-05	9.65E-03	9.99E-01	1.00E+00
Kirrel	1.07	2.75E-05	9.65E-03	9.99E-01	1.00E+00
Lta4h	1.07	3.59E-06	1.77E-03	9.99E-01	1.00E+00
Alkbh8	1.06	2.61E-05	9.47E-03	1.00E+00	1.00E+00
Cdc73	1.03	0.00011135	3.44E-02	9.95E-01	1.00E+00
Cdk12	1.02	1.84E-05	7.47E-03	1.00E+00	1.00E+00
Gosr2	1.02	0.00014583	4.19E-02	9.98E-01	1.00E+00
Rasa2	1.01	6.47E-06	2.97E-03	9.99E-01	1.00E+00
Senp1	0.99	0.00014583	4.19E-02	9.97E-01	1.00E+00
Fgf12	0.98	9.27E-05	2.95E-02	9.94E-01	1.00E+00
Creb3l2	0.98	6.15E-05	2.12E-02	9.97E-01	1.00E+00
Men1	0.96	2.08E-05	7.98E-03	9.99E-01	1.00E+00
Spop	0.96	1.51E-05	6.50E-03	9.99E-01	1.00E+00
Cbll1	0.91	0.00014439	4.19E-02	9.99E-01	1.00E+00
Ankrd24	0.90	1.75E-05	7.23E-03	9.98E-01	1.00E+00
Edem2	0.90	0.00016594	4.70E-02	9.98E-01	1.00E+00
Pcif1	0.87	2.42E-05	8.93E-03	9.98E-01	1.00E+00
4921507P07Rik	0.86	0.00017169	4.73E-02	9.93E-01	1.00E+00
Ddx42	0.85	1.20E-06	6.51E-04	9.79E-01	1.00E+00
Otud5	0.84	1.89E-05	7.52E-03	9.71E-01	1.00E+00
Dppa5a	0.84	1.13E-05	5.06E-03	9.96E-01	1.00E+00
Kif3a	0.77	0.00011949	3.63E-02	9.82E-01	1.00E+00
Sec22a	0.72	0.00014583	4.19E-02	9.92E-01	1.00E+00
Furin	0.71	0.00017648	4.80E-02	9.92E-01	1.00E+00

Ankrd6	0.49	7.40E-05	2.43E-02	7.32E-01	9.14E-01
Lsm12	0.29	6.44E-05	2.18E-02	4.65E-01	7.50E-01
Marcksl1	0.20	1.46E-05	6.43E-03	9.86E-02	4.84E-01
Atg3	-0.85	0.020985	4.20E-01	4.64E-04	4.63E-02
Dbp	-1.05	0.0016874	2.49E-01	2.59E-04	4.17E-02
Nln	-1.05	0.36437	1.00E+00	4.69E-04	4.63E-02
Xylb	-1.09	0.48935	1.00E+00	4.83E-04	4.63E-02
Pstpip2	-1.22	0.78233	1.00E+00	4.83E-04	4.63E-02
Olfr1463	-1.33	0.83086	1.00E+00	5.01E-04	4.63E-02
Pus7l	-1.37	0.79036	1.00E+00	2.74E-04	4.17E-02
Bpnt1	-1.45	0.24093	1.00E+00	3.10E-04	4.18E-02
Ttll5	-1.47	0.89188	1.00E+00	5.46E-04	4.63E-02
Olfr523	-1.47	0.5871	1.00E+00	2.89E-04	4.17E-02
Cyb5r2	-1.57	0.84605	1.00E+00	5.53E-04	4.63E-02
Crygc	-1.58	0.85002	1.00E+00	2.81E-04	4.17E-02
Phf12	-1.70	0.87576	1.00E+00	5.60E-04	4.63E-02
AI314180	-1.79	0.84838	1.00E+00	5.53E-04	4.63E-02
Pik3ca	-1.80	0.73094	1.00E+00	5.31E-04	4.63E-02
Sec23b	-1.80	0.77773	1.00E+00	4.83E-04	4.63E-02
Hagh	-1.83	0.42794	1.00E+00	4.71E-04	4.63E-02
Olfr237-ps1	-1.83	0.9129	1.00E+00	5.60E-04	4.63E-02
Tas2r104	-1.84	0.80913	1.00E+00	2.55E-04	4.17E-02
Erap1	-1.85	0.39007	1.00E+00	7.16E-05	2.00E-02
Sept3	-1.86	0.22664	1.00E+00	4.83E-04	4.63E-02
Zfand6	-1.89	0.97729	1.00E+00	5.55E-04	4.63E-02
C3ar1	-1.90	0.37623	1.00E+00	5.30E-04	4.63E-02
Mylip	-1.92	0.88336	1.00E+00	1.75E-04	3.68E-02
Gosr1	-1.92	0.99198	1.00E+00	1.85E-04	3.68E-02
Pcp4	-1.93	0.91935	1.00E+00	5.24E-04	4.63E-02
Cachd1	-1.95	0.81897	1.00E+00	1.80E-05	9.79E-03
Rfxap	-1.96	0.93257	1.00E+00	2.55E-04	4.17E-02
Slc12a2	-1.96	0.96301	1.00E+00	5.53E-04	4.63E-02
Ube2a	-1.97	0.8566	1.00E+00	4.66E-04	4.63E-02
Tgif2lx1	-1.98	0.95558	1.00E+00	5.06E-04	4.63E-02
Strn4	-1.98	0.9735	1.00E+00	5.46E-04	4.63E-02
Nudt11	-1.99	0.96227	1.00E+00	5.13E-04	4.63E-02
Tial1	-2.01	0.9539	1.00E+00	3.17E-04	4.18E-02
Tmem41b	-2.02	0.96579	1.00E+00	3.96E-04	4.63E-02

Lrrn3	-2.03	0.98067	1.00E+00	5.06E-04	4.63E-02
Tubb2b	-2.04	0.86216	1.00E+00	4.69E-04	4.63E-02
Gne	-2.06	0.95715	1.00E+00	5.45E-04	4.63E-02
Rsl1	-2.06	0.94016	1.00E+00	4.06E-04	4.63E-02
Zfp942	-2.07	0.97317	1.00E+00	4.12E-04	4.63E-02
Kmt2c	-2.08	0.59541	1.00E+00	4.83E-04	4.63E-02
Stat3	-2.08	0.99048	1.00E+00	4.06E-04	4.63E-02
Rgp1	-2.09	0.76343	1.00E+00	4.12E-04	4.63E-02
Ppp4r2	-2.11	0.95069	1.00E+00	2.80E-04	4.17E-02
Prdx1	-2.12	0.99041	1.00E+00	5.24E-04	4.63E-02
Pip5k1c	-2.12	0.99136	1.00E+00	2.55E-04	4.17E-02
Tmem165	-2.13	0.48032	1.00E+00	4.57E-04	4.63E-02
Carm1	-2.13	0.96937	1.00E+00	4.93E-04	4.63E-02
Vps16	-2.14	0.9762	1.00E+00	3.96E-04	4.63E-02
Rsph1	-2.15	0.97941	1.00E+00	2.89E-04	4.17E-02
Cd44	-2.15	0.98583	1.00E+00	2.63E-04	4.17E-02
Arf6	-2.16	0.95126	1.00E+00	2.59E-04	4.17E-02
Irgm2	-2.16	0.98195	1.00E+00	2.83E-04	4.17E-02
Lamtor1	-2.18	0.95816	1.00E+00	3.97E-04	4.63E-02
Cd36	-2.18	0.99451	1.00E+00	5.13E-04	4.63E-02
Zfp827	-2.19	0.98737	1.00E+00	4.69E-04	4.63E-02
Olfr512	-2.19	0.9518	1.00E+00	2.61E-05	1.02E-02
Nans	-2.20	0.97933	1.00E+00	5.53E-04	4.63E-02
Rnf38	-2.20	0.97671	1.00E+00	2.63E-04	4.17E-02
Eif2ak3	-2.20	0.99073	1.00E+00	5.13E-04	4.63E-02
Ikbkg	-2.21	0.9944	1.00E+00	2.08E-05	9.79E-03
Spen	-2.22	0.98152	1.00E+00	5.55E-04	4.63E-02
Ak2	-2.22	0.96937	1.00E+00	4.71E-04	4.63E-02
Icosl	-2.24	0.99186	1.00E+00	5.30E-04	4.63E-02
Krtap1-5	-2.24	0.98152	1.00E+00	1.56E-05	9.75E-03
Lemd2	-2.25	0.9933	1.00E+00	5.45E-04	4.63E-02
Gtf2i	-2.25	0.94313	1.00E+00	2.62E-04	4.17E-02
Xrcc2	-2.26	0.97576	1.00E+00	3.05E-04	4.18E-02
Bptf	-2.26	0.97193	1.00E+00	1.84E-04	3.68E-02
Impg1	-2.27	0.99352	1.00E+00	2.89E-04	4.17E-02
Birc2	-2.28	0.98877	1.00E+00	1.13E-04	2.86E-02
Batf2	-2.30	0.98999	1.00E+00	2.58E-04	4.17E-02
Larp4	-2.30	0.97355	1.00E+00	2.55E-04	4.17E-02
Cwf19l1	-2.30	0.91546	1.00E+00	4.83E-04	4.63E-02

Tgtp1	-2.30	0.90076	1.00E+00	7.30E-05	2.00E-02
Pak2	-2.30	0.9912	1.00E+00	5.46E-04	4.63E-02
Ube2k	-2.32	0.99548	1.00E+00	3.17E-04	4.18E-02
Faxc	-2.33	0.99186	1.00E+00	2.59E-04	4.17E-02
Asxl2	-2.33	0.9296	1.00E+00	1.82E-04	3.68E-02
Matr3	-2.33	0.97193	1.00E+00	5.01E-04	4.63E-02
Rab7	-2.34	0.98577	1.00E+00	5.45E-04	4.63E-02
Arl14epl	-2.34	0.99093	1.00E+00	3.03E-04	4.18E-02
Tm2d1	-2.34	0.99258	1.00E+00	2.81E-04	4.17E-02
Uba6	-2.35	0.9925	1.00E+00	5.46E-04	4.63E-02
Fam234b	-2.35	0.72319	1.00E+00	7.06E-05	2.00E-02
Rsf1	-2.35	0.99657	1.00E+00	4.83E-04	4.63E-02
Hes7	-2.36	0.89628	1.00E+00	2.55E-04	4.17E-02
Hsd17b4	-2.36	0.98272	1.00E+00	1.13E-04	2.86E-02
Gpx4	-2.36	0.99594	1.00E+00	5.24E-04	4.63E-02
Txndc15	-2.37	0.92739	1.00E+00	4.83E-04	4.63E-02
Cdk2	-2.37	0.99215	1.00E+00	2.83E-04	4.17E-02
Pigu	-2.37	0.99418	1.00E+00	2.83E-04	4.17E-02
Rfx6	-2.37	0.99498	1.00E+00	5.46E-04	4.63E-02
Padi4	-2.38	0.99068	1.00E+00	3.10E-04	4.18E-02
Ube2r2	-2.38	0.98387	1.00E+00	5.46E-04	4.63E-02
Fhod3	-2.39	0.98998	1.00E+00	1.68E-04	3.68E-02
Ice1	-2.39	0.99477	1.00E+00	4.83E-04	4.63E-02
Xrcc4	-2.39	0.90778	1.00E+00	2.69E-04	4.17E-02
Foxb1	-2.39	0.99902	1.00E+00	5.55E-04	4.63E-02
Stub1	-2.39	0.98149	1.00E+00	2.58E-04	4.17E-02
Ccdc137	-2.39	0.98149	1.00E+00	4.66E-04	4.63E-02
Snapin	-2.40	0.97303	1.00E+00	7.11E-05	2.00E-02
Trip13	-2.40	0.99343	1.00E+00	5.56E-04	4.63E-02
Nckap1	-2.42	0.9851	1.00E+00	1.85E-04	3.68E-02
Gml	-2.42	0.98162	1.00E+00	1.85E-04	3.68E-02
Ube2j2	-2.42	0.99665	1.00E+00	3.18E-04	4.18E-02
Nsdhl	-2.42	0.99658	1.00E+00	5.53E-04	4.63E-02
Arid4a	-2.43	0.80658	1.00E+00	1.84E-05	9.79E-03
Galnt15	-2.43	0.99902	1.00E+00	5.13E-04	4.63E-02
Rab13	-2.44	0.99042	1.00E+00	4.83E-04	4.63E-02
Gigyf2	-2.44	0.99705	1.00E+00	2.81E-04	4.17E-02
Ero1l	-2.44	0.99887	1.00E+00	5.06E-04	4.63E-02
Olfr912	-2.45	0.99066	1.00E+00	5.13E-04	4.63E-02

Zc3h18	-2.45	0.99723	1.00E+00	4.68E-04	4.63E-02
Nfix	-2.45	0.9959	1.00E+00	2.08E-05	9.79E-03
Neurl3	-2.45	0.99577	1.00E+00	5.01E-04	4.63E-02
Hspa13	-2.46	0.99844	1.00E+00	5.13E-04	4.63E-02
Xrcc5	-2.46	0.9979	1.00E+00	1.75E-04	3.68E-02
Prl2c3	-2.47	0.99614	1.00E+00	1.75E-04	3.68E-02
Keap1	-2.47	0.98993	1.00E+00	1.13E-04	2.86E-02
Pax3	-2.47	0.99466	1.00E+00	2.92E-04	4.18E-02
Ankrd11	-2.47	0.98473	1.00E+00	2.80E-04	4.17E-02
Atg16l1	-2.48	0.99847	1.00E+00	5.60E-04	4.63E-02
Oprk1	-2.48	0.99358	1.00E+00	5.24E-04	4.63E-02
Sox11	-2.48	0.98494	1.00E+00	2.80E-04	4.17E-02
Ttc33	-2.48	0.99723	1.00E+00	2.83E-04	4.17E-02
Tbc1d10b	-2.48	0.98395	1.00E+00	2.55E-04	4.17E-02
Arhgap11a	-2.49	0.99723	1.00E+00	4.90E-04	4.63E-02
Ar	-2.49	0.99435	1.00E+00	2.67E-04	4.17E-02
Arhgap21	-2.50	0.99764	1.00E+00	2.83E-04	4.17E-02
Rfwd2	-2.51	0.99466	1.00E+00	4.83E-04	4.63E-02
Crlf3	-2.52	0.99906	1.00E+00	4.11E-04	4.63E-02
Elmo2	-2.52	0.99593	1.00E+00	3.12E-04	4.18E-02
Tgif2	-2.53	0.99901	1.00E+00	5.60E-04	4.63E-02
Sod2	-2.53	0.99643	1.00E+00	4.69E-04	4.63E-02
Fam170b	-2.54	0.9833	1.00E+00	1.13E-04	2.86E-02
Xrcc1	-2.54	0.99811	1.00E+00	3.12E-04	4.18E-02
Meioc	-2.54	0.99689	1.00E+00	3.17E-04	4.18E-02
March5	-2.55	0.99799	1.00E+00	7.90E-06	7.00E-03
Pitx2	-2.56	0.99902	1.00E+00	3.12E-04	4.18E-02
Rab25	-2.56	0.99719	1.00E+00	5.13E-04	4.63E-02
Ccdc155	-2.56	0.99257	1.00E+00	7.16E-05	2.00E-02
Zfp473	-2.56	0.99762	1.00E+00	4.12E-04	4.63E-02
Tbk1	-2.58	0.99959	1.00E+00	4.57E-04	4.63E-02
Zfp148	-2.58	0.99863	1.00E+00	5.60E-04	4.63E-02
Rgmb	-2.58	0.99711	1.00E+00	4.79E-04	4.63E-02
Tm2d3	-2.59	0.98635	1.00E+00	7.16E-05	2.00E-02
Tsc2	-2.59	0.99145	1.00E+00	4.56E-04	4.63E-02
2700049A03Rik	-2.59	0.99917	1.00E+00	4.00E-04	4.63E-02
Cdk5	-2.60	0.99621	1.00E+00	4.90E-04	4.63E-02
Cmip	-2.60	0.99622	1.00E+00	4.12E-04	4.63E-02
Ccdc187	-2.60	0.99705	1.00E+00	2.80E-04	4.17E-02

Cnot8	-2.60	0.99918	1.00E+00	3.10E-04	4.18E-02
Dspp	-2.60	0.99548	1.00E+00	3.12E-04	4.18E-02
Ywhaz	-2.60	0.99438	1.00E+00	7.26E-05	2.00E-02
Cfhr2	-2.61	0.9925	1.00E+00	7.16E-05	2.00E-02
Zfp281	-2.61	0.99865	1.00E+00	6.97E-05	2.00E-02
Becn1	-2.61	0.99906	1.00E+00	2.69E-04	4.17E-02
Slc2a1	-2.61	0.99946	1.00E+00	7.21E-05	2.00E-02
Ilk	-2.62	0.9989	1.00E+00	4.83E-04	4.63E-02
Gpr31b	-2.62	0.99422	1.00E+00	2.56E-05	1.02E-02
Sprr2e	-2.62	0.99665	1.00E+00	5.24E-04	4.63E-02
Boll	-2.63	0.99136	1.00E+00	2.56E-05	1.02E-02
Tacc3	-2.63	0.99846	1.00E+00	2.55E-04	4.17E-02
Paox	-2.66	0.99923	1.00E+00	5.00E-04	4.63E-02
Gabrb3	-2.66	0.99887	1.00E+00	2.59E-04	4.17E-02
Trex1	-2.67	0.99964	1.00E+00	5.24E-04	4.63E-02
Dnaja2	-2.67	0.99907	1.00E+00	5.53E-04	4.63E-02
Vps4b	-2.68	0.9981	1.00E+00	5.46E-04	4.63E-02
Nprl3	-2.68	0.99974	1.00E+00	4.90E-04	4.63E-02
Mtch1	-2.68	0.99534	1.00E+00	7.16E-05	2.00E-02
Iqsec1	-2.68	0.89653	1.00E+00	7.42E-06	7.00E-03
Lrp10	-2.68	0.99784	1.00E+00	7.21E-05	2.00E-02
Raf1	-2.69	0.99392	1.00E+00	1.74E-04	3.68E-02
Dtx3l	-2.69	0.999	1.00E+00	1.13E-04	2.86E-02
Ccs	-2.70	0.99858	1.00E+00	1.68E-04	3.68E-02
Epc1	-2.70	0.99881	1.00E+00	2.74E-04	4.17E-02
Strada	-2.70	0.9977	1.00E+00	1.68E-04	3.68E-02
Nrbf2	-2.70	0.99964	1.00E+00	4.83E-04	4.63E-02
Ten1	-2.72	0.99964	1.00E+00	7.11E-05	2.00E-02
Irf1	-2.72	0.999	1.00E+00	7.21E-05	2.00E-02
Vmn2r72	-2.72	0.99853	1.00E+00	1.74E-04	3.68E-02
Tk2	-2.73	0.99964	1.00E+00	4.63E-04	4.63E-02
Ddi2	-2.73	0.99216	1.00E+00	1.46E-05	9.44E-03
Arid1a	-2.74	0.99903	1.00E+00	7.21E-05	2.00E-02
Zfp273	-2.75	0.99863	1.00E+00	1.75E-04	3.68E-02
Actr3	-2.75	0.99505	1.00E+00	1.75E-05	9.79E-03
Eif2ak4	-2.75	0.99846	1.00E+00	2.56E-05	1.02E-02
Pde7a	-2.76	0.99715	1.00E+00	1.62E-04	3.68E-02
Dpf2	-2.76	0.99881	1.00E+00	1.85E-04	3.68E-02
Rraga	-2.76	0.99382	1.00E+00	1.13E-04	2.86E-02

Rnf31	-2.77	0.99534	1.00E+00	1.74E-04	3.68E-02
Smgc	-2.78	0.99719	1.00E+00	2.56E-05	1.02E-02
Prkcq	-2.79	0.99731	1.00E+00	1.68E-04	3.68E-02
Epg5	-2.79	0.99622	1.00E+00	7.06E-05	2.00E-02
Gss	-2.79	0.99969	1.00E+00	2.74E-04	4.17E-02
Cnot11	-2.80	0.99704	1.00E+00	1.68E-04	3.68E-02
Hipk2	-2.80	0.99722	1.00E+00	2.51E-05	1.02E-02
C330027C09Rik	-2.80	0.99439	1.00E+00	1.80E-05	9.79E-03
Man2a1	-2.80	0.99812	1.00E+00	2.04E-05	9.79E-03
Chmp5	-2.82	0.99418	1.00E+00	7.90E-06	7.00E-03
Pcgf6	-2.86	0.99811	1.00E+00	9.34E-06	7.00E-03
Nampt	-2.87	0.99887	1.00E+00	2.54E-04	4.17E-02
Eri1	-2.88	0.99964	1.00E+00	2.67E-04	4.17E-02
Pbrm1	-2.89	0.99881	1.00E+00	8.38E-06	7.00E-03
Atg5	-2.89	0.99974	1.00E+00	4.12E-04	4.63E-02
Ube2h	-2.90	0.99771	1.00E+00	9.34E-06	7.00E-03
Gabpb1	-2.91	0.99907	1.00E+00	7.06E-05	2.00E-02
Gpi1	-2.91	0.9971	1.00E+00	1.41E-05	9.42E-03
Usp19	-2.92	0.99969	1.00E+00	1.81E-04	3.68E-02
Brd7	-2.94	0.99974	1.00E+00	1.68E-04	3.68E-02
Jmjd6	-2.95	0.99505	1.00E+00	1.41E-05	9.42E-03
Tgif1	-2.97	0.99906	1.00E+00	7.11E-05	2.00E-02
Fis1	-2.98	0.99995	1.00E+00	1.85E-04	3.68E-02
Cflar	-2.98	0.99875	1.00E+00	7.21E-05	2.00E-02
Ptpn11	-2.99	0.99917	1.00E+00	7.42E-06	7.00E-03
Maea	-3.00	0.99946	1.00E+00	6.97E-05	2.00E-02
Hdac5	-3.00	0.99969	1.00E+00	2.04E-05	9.79E-03
Mprip	-3.01	0.99923	1.00E+00	9.82E-06	7.00E-03
Itgav	-3.02	0.99936	1.00E+00	7.21E-05	2.00E-02
Crkl	-3.06	0.99974	1.00E+00	2.56E-05	1.02E-02
Arid2	-3.06	0.99902	1.00E+00	1.89E-05	9.79E-03
Memo1	-3.07	0.99995	1.00E+00	7.26E-05	2.00E-02
Serpinb9	-3.08	0.99831	1.00E+00	2.04E-05	9.79E-03
Krit1	-3.08	0.99902	1.00E+00	9.82E-06	7.00E-03
Srrd	-3.13	0.99964	1.00E+00	9.34E-06	7.00E-03
Sox4	-3.17	0.99996	1.00E+00	1.75E-05	9.79E-03
Wdr26	-3.17	0.99969	1.00E+00	2.61E-05	1.02E-02
Tiparp	-3.18	0.99969	1.00E+00	9.34E-06	7.00E-03
Nadk	-3.18	0.99764	1.00E+00	1.20E-06	3.54E-03

Tk1	-3.18	0.99974	1.00E+00	7.90E-06	7.00E-03
Tcof1	-3.20	0.99865	1.00E+00	7.90E-06	7.00E-03
Nprl2	-3.20	0.99969	1.00E+00	9.34E-06	7.00E-03
Ptpn2	-3.22	0.99902	1.00E+00	8.38E-06	7.00E-03
Gale	-3.22	0.99996	1.00E+00	7.35E-05	2.00E-02
Spns1	-3.24	0.99995	1.00E+00	2.56E-05	1.02E-02
Usp18	-3.28	0.99964	1.00E+00	1.68E-06	4.33E-03
Psme2	-3.29	0.99974	1.00E+00	7.42E-06	7.00E-03
Tcea1	-3.31	0.99925	1.00E+00	1.20E-06	3.54E-03
Fitm2	-3.33	0.99917	1.00E+00	7.42E-06	7.00E-03
Ypel5	-3.36	0.9993	1.00E+00	7.90E-06	7.00E-03
Creb1	-3.40	0.99964	1.00E+00	7.42E-06	7.00E-03
Rela	-3.45	0.99924	1.00E+00	2.39E-07	1.24E-03
Fadd	-3.45	0.99995	1.00E+00	7.42E-06	7.00E-03
Psme1	-3.53	0.99996	1.00E+00	7.42E-06	7.00E-03
Ikbkb	-3.57	1	1.00E+00	1.20E-06	3.54E-03
Cd274	-3.70	0.99995	1.00E+00	2.39E-07	1.24E-03
Otulin	-3.73	0.99995	1.00E+00	2.39E-07	1.24E-03
Psmb8	-3.93	1	1.00E+00	2.39E-07	1.24E-03

Table.S2 Complete list of top candidate genes in OT-I screen (FDR<0.05).

LogFC, Log2 fold change; FDR, False Discovery rate. FDR and p value calculated by MaGeCK.

		Positive selection		Negative selection	
Gene	**logFC**	**p value**	**FDR**	**p value**	**FDR**
B2m	5.36	2.39E-07	3.81E-04	1.00E+00	1.00E+00
Ifngr2	3.53	2.39E-07	3.81E-04	1.00E+00	1.00E+00
Ifngr1	3.44	2.39E-07	3.81E-04	1.00E+00	1.00E+00
Jak2	3.10	2.39E-07	3.81E-04	1.00E+00	1.00E+00
Setd2	2.72	2.39E-07	3.81E-04	1.00E+00	1.00E+00
Jak1	2.50	2.39E-07	3.81E-04	1.00E+00	1.00E+00
Stat1	2.44	2.39E-07	3.81E-04	1.00E+00	1.00E+00
Kmt2b	1.82	2.39E-07	3.81E-04	1.00E+00	1.00E+00
Alad	1.38	2.39E-07	3.81E-04	1.00E+00	1.00E+00
Wdr48	1.37	2.39E-07	3.81E-04	9.99E-01	1.00E+00
Wdr20	1.34	2.39E-07	3.81E-04	1.00E+00	1.00E+00
Nf1	1.27	2.39E-07	3.81E-04	9.99E-01	1.00E+00
Cs	1.20	7.18E-07	1.06E-03	1.00E+00	1.00E+00
Ubr5	1.15	4.96E-05	4.66E-02	1.00E+00	1.00E+00
Kctd5	1.07	2.39E-07	3.81E-04	9.96E-01	1.00E+00
Hnrnph1	1.06	1.17E-05	1.43E-02	9.99E-01	1.00E+00
Wdr24	1.04	3.59E-06	4.95E-03	9.97E-01	1.00E+00
Olfr600	0.99	3.28E-05	3.23E-02	9.90E-01	1.00E+00
Lrrc8a	0.91	3.23E-05	3.23E-02	9.99E-01	1.00E+00
Naa30	0.89	1.46E-05	1.68E-02	9.97E-01	1.00E+00
Sult6b1	0.86	8.86E-06	1.14E-02	9.81E-01	1.00E+00
Cep57l1	0.84	2.47E-05	2.68E-02	9.90E-01	1.00E+00
Olfr1450	-1.38	9.01E-01	1.00E+00	1.42E-04	3.41E-02
Pstpip2	-1.53	9.83E-01	1.00E+00	2.56E-04	4.22E-02
Lrrtm4	-1.55	9.62E-01	1.00E+00	2.96E-04	4.22E-02
Nmt2	-1.58	5.03E-01	1.00E+00	2.71E-04	4.22E-02
Lamtor4	-1.59	9.74E-01	1.00E+00	8.02E-05	2.15E-02
Tert	-1.61	8.82E-01	1.00E+00	3.02E-04	4.22E-02
Rce1	-1.63	8.71E-01	1.00E+00	2.33E-04	4.19E-02
Socs1	-1.64	1.38E-01	9.49E-01	8.07E-05	2.15E-02
Ropn1	-1.64	2.64E-01	1.00E+00	2.44E-04	4.22E-02
Alk	-1.64	5.06E-01	1.00E+00	8.21E-05	2.15E-02
Ctps	-1.69	9.67E-01	1.00E+00	2.16E-04	4.11E-02
Mogs	-1.71	9.75E-01	1.00E+00	2.20E-04	4.11E-02
Rars2	-1.72	9.66E-01	1.00E+00	2.16E-04	4.11E-02

Vmn1r2	-1.74	9.83E-01	1.00E+00	3.02E-04	4.22E-02
Gpx1	-1.74	5.03E-01	1.00E+00	2.51E-04	4.22E-02
Pdzph1	-1.75	9.13E-01	1.00E+00	8.07E-05	2.15E-02
Rwdd1	-1.76	9.81E-01	1.00E+00	2.63E-04	4.22E-02
Med23	-1.77	5.68E-01	1.00E+00	2.47E-04	4.22E-02
Rpl22l1	-1.80	5.92E-01	1.00E+00	2.96E-04	4.22E-02
B3glct	-1.82	8.87E-01	1.00E+00	3.76E-05	1.65E-02
Hsd17b10	-1.83	9.88E-01	1.00E+00	2.21E-04	4.11E-02
Kctd2	-1.85	9.85E-01	1.00E+00	1.42E-04	3.41E-02
Slc33a1	-1.86	9.73E-01	1.00E+00	9.27E-05	2.37E-02
Pak2	-1.86	9.77E-01	1.00E+00	2.85E-04	4.22E-02
Atf4	-1.87	9.85E-01	1.00E+00	8.07E-05	2.15E-02
Scyl1	-1.88	9.89E-01	1.00E+00	2.86E-04	4.22E-02
Gramd1b	-1.90	9.75E-01	1.00E+00	2.43E-04	4.22E-02
Rnd2	-1.91	7.48E-01	1.00E+00	2.96E-04	4.22E-02
Olfr220	-1.91	9.79E-01	1.00E+00	2.96E-04	4.22E-02
Olfr969	-1.91	8.31E-01	1.00E+00	2.96E-04	4.22E-02
Osgepl1	-1.91	9.40E-01	1.00E+00	2.21E-04	4.11E-02
Rbbp4	-1.92	9.89E-01	1.00E+00	2.16E-04	4.11E-02
Alg3	-1.94	9.88E-01	1.00E+00	3.08E-04	4.22E-02
Rbck1	-1.96	9.30E-01	1.00E+00	2.85E-05	1.65E-02
Ylpm1	-1.97	5.12E-01	1.00E+00	2.86E-04	4.22E-02
Ssu72	-1.98	9.88E-01	1.00E+00	2.75E-04	4.22E-02
Cyld	-1.98	9.94E-01	1.00E+00	2.16E-04	4.11E-02
Mc1r	-1.99	9.90E-01	1.00E+00	8.07E-05	2.15E-02
Anp32b	-1.99	9.97E-01	1.00E+00	2.47E-04	4.22E-02
Ccs	-1.99	9.94E-01	1.00E+00	2.85E-04	4.22E-02
Hsd17b12	-2.00	9.88E-01	1.00E+00	2.37E-04	4.22E-02
Prl2c3	-2.01	9.97E-01	1.00E+00	1.53E-04	3.50E-02
Ankrd46	-2.02	9.90E-01	1.00E+00	2.16E-04	4.11E-02
Ikbkg	-2.03	9.98E-01	1.00E+00	3.08E-04	4.22E-02
Ddx20	-2.03	9.89E-01	1.00E+00	2.85E-04	4.22E-02
Akt1	-2.04	6.94E-01	1.00E+00	2.16E-04	4.11E-02
Exoc7	-2.05	9.85E-01	1.00E+00	8.07E-05	2.15E-02
Larp4	-2.06	9.88E-01	1.00E+00	2.24E-04	4.11E-02
Ubtd1	-2.07	9.71E-01	1.00E+00	1.42E-04	3.41E-02
Brwd3	-2.09	9.92E-01	1.00E+00	3.08E-04	4.22E-02
Nudcd2	-2.09	9.98E-01	1.00E+00	8.02E-05	2.15E-02
Ppcs	-2.09	9.88E-01	1.00E+00	1.40E-04	3.41E-02

Mrps21	-2.09	9.99E-01	1.00E+00	2.24E-04	4.11E-02
Gnb2	-2.09	9.88E-01	1.00E+00	7.40E-05	2.15E-02
Chic2	-2.09	9.95E-01	1.00E+00	3.90E-05	1.65E-02
Fnbp4	-2.09	9.98E-01	1.00E+00	2.16E-04	4.11E-02
Plpp2	-2.10	9.93E-01	1.00E+00	2.85E-04	4.22E-02
Trip11	-2.11	9.99E-01	1.00E+00	2.96E-04	4.22E-02
Ccna2	-2.12	9.89E-01	1.00E+00	1.53E-04	3.50E-02
Brinp2	-2.12	9.97E-01	1.00E+00	2.86E-04	4.22E-02
Hnrnpf	-2.12	9.84E-01	1.00E+00	3.57E-05	1.65E-02
Ccdc134	-2.12	9.99E-01	1.00E+00	3.90E-05	1.65E-02
Prdm10	-2.14	9.83E-01	1.00E+00	2.80E-05	1.65E-02
Smarce1	-2.15	9.88E-01	1.00E+00	7.06E-05	2.15E-02
Tmed2	-2.15	9.97E-01	1.00E+00	2.75E-04	4.22E-02
Usp24	-2.15	9.99E-01	1.00E+00	3.02E-04	4.22E-02
Ipo11	-2.17	9.95E-01	1.00E+00	2.96E-04	4.22E-02
Arf6	-2.18	9.94E-01	1.00E+00	2.96E-04	4.22E-02
Prrc2a	-2.19	9.98E-01	1.00E+00	2.20E-04	4.11E-02
Rhbdl2	-2.19	9.97E-01	1.00E+00	2.10E-04	4.11E-02
Lman2	-2.20	9.93E-01	1.00E+00	3.67E-04	4.99E-02
Parn	-2.22	9.97E-01	1.00E+00	9.27E-05	2.37E-02
Tvp23b	-2.24	9.98E-01	1.00E+00	2.16E-04	4.11E-02
Vmn1r167	-2.25	7.30E-01	1.00E+00	8.12E-05	2.15E-02
Med7	-2.25	9.98E-01	1.00E+00	7.73E-05	2.15E-02
Prkcq	-2.26	9.97E-01	1.00E+00	8.07E-05	2.15E-02
Gne	-2.27	9.97E-01	1.00E+00	8.02E-05	2.15E-02
Aip	-2.27	9.99E-01	1.00E+00	8.07E-05	2.15E-02
Crocc	-2.27	9.97E-01	1.00E+00	8.02E-05	2.15E-02
Uggt1	-2.31	9.98E-01	1.00E+00	3.02E-04	4.22E-02
Atr	-2.32	9.95E-01	1.00E+00	7.45E-05	2.15E-02
Ccnc	-2.33	9.99E-01	1.00E+00	2.20E-04	4.11E-02
Rer1	-2.34	9.93E-01	1.00E+00	7.40E-05	2.15E-02
Cks1b	-2.34	9.94E-01	1.00E+00	7.90E-06	7.22E-03
Ptar1	-2.35	9.98E-01	1.00E+00	3.71E-05	1.65E-02
Dlst	-2.35	9.92E-01	1.00E+00	2.80E-05	1.65E-02
Ubr4	-2.35	9.97E-01	1.00E+00	3.86E-05	1.65E-02
Ddx42	-2.35	9.89E-01	1.00E+00	8.38E-06	7.22E-03
C330007P06Rik	-2.35	9.99E-01	1.00E+00	2.69E-04	4.22E-02
Vps29	-2.37	9.98E-01	1.00E+00	8.07E-05	2.15E-02
Atg13	-2.37	1.00E+00	1.00E+00	2.88E-04	4.22E-02

Rab1a	-2.39	1.00E+00	1.00E+00	1.53E-04	3.50E-02
Rad51d	-2.39	9.97E-01	1.00E+00	4.19E-05	1.67E-02
Otulin	-2.39	9.99E-01	1.00E+00	2.16E-04	4.11E-02
Gpaa1	-2.40	9.99E-01	1.00E+00	8.02E-05	2.15E-02
Pih1d1	-2.41	9.98E-01	1.00E+00	8.02E-05	2.15E-02
Nrbf2	-2.41	8.58E-01	1.00E+00	8.07E-05	2.15E-02
BC030336	-2.42	9.89E-01	1.00E+00	7.90E-06	7.22E-03
Nepro	-2.43	9.96E-01	1.00E+00	2.16E-04	4.11E-02
Rbm34	-2.44	9.90E-01	1.00E+00	6.47E-06	7.22E-03
Ireb2	-2.44	9.98E-01	1.00E+00	2.16E-04	4.11E-02
Sgol1	-2.44	9.98E-01	1.00E+00	1.53E-04	3.50E-02
Ugp2	-2.45	9.99E-01	1.00E+00	2.29E-04	4.15E-02
Arf3	-2.46	9.99E-01	1.00E+00	2.16E-04	4.11E-02
Itgav	-2.47	9.98E-01	1.00E+00	3.86E-05	1.65E-02
Ube2n	-2.47	9.96E-01	1.00E+00	3.62E-05	1.65E-02
Mcl1	-2.48	9.99E-01	1.00E+00	1.42E-04	3.41E-02
Map3k7	-2.48	9.98E-01	1.00E+00	3.57E-05	1.65E-02
Vps11	-2.49	9.99E-01	1.00E+00	2.16E-04	4.11E-02
Birc2	-2.49	1.00E+00	1.00E+00	3.62E-05	1.65E-02
Vmn1r202	-2.50	9.99E-01	1.00E+00	2.71E-04	4.22E-02
Rela	-2.51	9.99E-01	1.00E+00	2.16E-04	4.11E-02
N4bp1	-2.54	9.99E-01	1.00E+00	2.80E-05	1.65E-02
Slc35a1	-2.55	9.96E-01	1.00E+00	6.47E-06	7.22E-03
Gm7534	-2.57	9.99E-01	1.00E+00	3.86E-05	1.65E-02
Tmed10	-2.58	9.99E-01	1.00E+00	8.02E-05	2.15E-02
Tlcd1	-2.58	1.00E+00	1.00E+00	8.07E-05	2.15E-02
Sptlc2	-2.62	9.97E-01	1.00E+00	6.94E-06	7.22E-03
Sepsecs	-2.62	9.98E-01	1.00E+00	4.19E-05	1.67E-02
Pigk	-2.62	9.99E-01	1.00E+00	6.94E-06	7.22E-03
Sptlc1	-2.64	9.97E-01	1.00E+00	3.14E-05	1.65E-02
Asnsd1	-2.65	9.99E-01	1.00E+00	3.86E-05	1.65E-02
Gpx4	-2.65	9.99E-01	1.00E+00	8.07E-05	2.15E-02
Uba6	-2.66	9.99E-01	1.00E+00	7.02E-05	2.15E-02
Vps33a	-2.67	1.00E+00	1.00E+00	7.42E-06	7.22E-03
Tmx2	-2.67	9.99E-01	1.00E+00	8.38E-06	7.22E-03
Cwc27	-2.68	9.95E-01	1.00E+00	1.92E-06	5.45E-03
Chtf8	-2.69	1.00E+00	1.00E+00	7.45E-05	2.15E-02
Kmt2d	-2.69	9.99E-01	1.00E+00	3.76E-05	1.65E-02
Atg5	-2.69	9.98E-01	1.00E+00	3.90E-05	1.65E-02

Dscc1	-2.70	9.97E-01	1.00E+00	2.63E-06	5.45E-03
Atp6v1h	-2.71	9.98E-01	1.00E+00	6.94E-06	7.22E-03
Slc7a11	-2.73	9.99E-01	1.00E+00	3.71E-05	1.65E-02
Gss	-2.74	1.00E+00	1.00E+00	2.21E-04	4.11E-02
Pigu	-2.78	1.00E+00	1.00E+00	2.63E-06	5.45E-03
Stub1	-2.79	9.97E-01	1.00E+00	7.18E-07	4.95E-03
Calr	-2.82	9.99E-01	1.00E+00	2.85E-05	1.65E-02
Aprt	-2.83	9.99E-01	1.00E+00	2.80E-05	1.65E-02
Alg8	-2.84	9.99E-01	1.00E+00	2.16E-06	5.45E-03
Ei24	-2.85	1.00E+00	1.00E+00	4.14E-05	1.67E-02
Mtch1	-2.87	9.99E-01	1.00E+00	7.90E-06	7.22E-03
Eefsec	-2.91	9.97E-01	1.00E+00	2.39E-07	2.48E-03
Traf3	-2.94	1.00E+00	1.00E+00	7.90E-06	7.22E-03
Usp18	-2.95	9.99E-01	1.00E+00	3.71E-05	1.65E-02
Vps4b	-2.97	1.00E+00	1.00E+00	2.90E-05	1.65E-02
Traf2	-2.98	1.00E+00	1.00E+00	6.47E-06	7.22E-03
Pigs	-3.01	1.00E+00	1.00E+00	2.75E-05	1.65E-02
Fitm2	-3.03	1.00E+00	1.00E+00	2.63E-06	5.45E-03
Megf8	-3.14	1.00E+00	1.00E+00	2.16E-06	5.45E-03
Eri1	-3.18	1.00E+00	1.00E+00	6.47E-06	7.22E-03
Rnf31	-3.40	1.00E+00	1.00E+00	2.16E-06	5.45E-03
Ptpn2	-3.63	1.00E+00	1.00E+00	2.39E-07	2.48E-03

Table. S3 Gene sets (Hallmark and KEGG gene sets) significantly enriched (FDR<0.05) in Pmel-1 or OT-I screens.

Gene sets related to Fig.1D were highlighted.

Gene Set Name	Screen	p-value	q-value
KEGG_JAK_STAT_SIGNALING_PATHWAY	Pmel1	8.69E-11	2.36E-08
HALLMARK_ALLOGRAFT_REJECTION	Pmel1	6.61E-10	8.99E-08
KEGG_LEISHMANIA_INFECTION	Pmel1	1.21E-09	1.41E-07
HALLMARK_INTERFERON_GAMMA_RESPONSE	Pmel1	2.06E-08	1.68E-06
HALLMARK_IL6_JAK_STAT3_SIGNALING	Pmel1	8.89E-06	4.84E-04
KEGG_ANTIGEN_PROCESSING_AND_PRESENTATION	Pmel1	9.73E-06	4.96E-04
KEGG_PRIMARY_IMMUNODEFICIENCY	Pmel1	1.96E-05	8.89E-04
KEGG_NATURAL_KILLER_CELL_MEDIATED_CYTOTOXICITY	Pmel1	5.31E-05	2.17E-03
HALLMARK_COMPLEMENT	Pmel1	2.28E-04	6.00E-03
HALLMARK_INFLAMMATORY_RESPONSE	Pmel1	2.28E-04	6.00E-03
KEGG_TOLL_LIKE_RECEPTOR_SIGNALING_PATHWAY	Pmel1	4.79E-04	1.12E-02
KEGG_CYTOKINE_CYTOKINE_RECEPTOR_INTERACTION	Pmel1	6.78E-04	1.47E-02
KEGG_MAPK_SIGNALING_PATHWAY	Pmel1	6.78E-04	1.47E-02
KEGG_UBIQUITIN_MEDIATED_PROTEOLYSIS	Pmel1	1.15E-03	2.13E-02
KEGG_PATHWAYS_IN_CANCER	Pmel1	1.45E-03	2.63E-02
HALLMARK_APOPTOSIS	Pmel1	1.79E-03	3.10E-02
KEGG_LEISHMANIA_INFECTION	OT-I	1.25E-10	1.02E-07
KEGG_JAK_STAT_SIGNALING_PATHWAY	OT-I	6.09E-09	2.48E-06
HALLMARK_ALLOGRAFT_REJECTION	OT-I	2.18E-08	5.94E-06
HALLMARK_IL6_JAK_STAT3_SIGNALING	OT-I	7.30E-06	1.49E-03
HALLMARK_INTERFERON_GAMMA_RESPONSE	OT-I	8.76E-05	8.94E-03
KEGG_PANCREATIC_CANCER	OT-I	4.27E-04	3.87E-02

Table. S4 Gene sets (Hallmark and KEGG gene sets) significantly depleted (LFC>2, FDR q<0.05) in Pmel-1 or OT-I screens.

Gene sets related to Fig.1D were highlighted.

Gene Set Name	Screen	p-value	q-value
HALLMARK_INTERFERON_GAMMA_RESPONSE	Pmel1	4.00E-11	9.44E-09
KEGG_ADIPOCYTOKINE_SIGNALING_PATHWAY	Pmel1	3.15E-10	3.72E-08
KEGG_UBIQUITIN_MEDIATED_PROTEOLYSIS	Pmel1	5.60E-09	4.40E-07
HALLMARK_TNFA_SIGNALING_VIA_NFKB	Pmel1	1.02E-08	4.66E-07
KEGG_PATHWAYS_IN_CANCER	Pmel1	1.11E-08	4.66E-07
HALLMARK_PI3K_AKT_MTOR_SIGNALING	Pmel1	1.18E-08	4.66E-07
KEGG_PROSTATE_CANCER	Pmel1	7.97E-08	2.69E-06
HALLMARK_INTERFERON_ALPHA_RESPONSE	Pmel1	1.45E-07	4.27E-06
KEGG_RIG_I_LIKE_RECEPTOR_SIGNALING_PATHWAY	Pmel1	4.52E-07	1.19E-05
KEGG_CHRONIC_MYELOID_LEUKEMIA	Pmel1	5.34E-07	1.26E-05
KEGG_SMALL_CELL_LUNG_CANCER	Pmel1	1.23E-06	2.64E-05
HALLMARK_IL6_JAK_STAT3_SIGNALING	Pmel1	1.51E-06	2.85E-05
KEGG_APOPTOSIS	Pmel1	1.62E-06	2.85E-05
HALLMARK_MTORC1_SIGNALING	Pmel1	1.69E-06	2.85E-05
KEGG_CYTOSOLIC_DNA_SENSING_PATHWAY	Pmel1	3.24E-06	5.10E-05
HALLMARK_APOPTOSIS	Pmel1	4.42E-06	6.34E-05
KEGG_ACUTE_MYELOID_LEUKEMIA	Pmel1	4.57E-06	6.34E-05
KEGG_T_CELL_RECEPTOR_SIGNALING_PATHWAY	Pmel1	5.34E-06	7.00E-05
KEGG_PANCREATIC_CANCER	Pmel1	9.80E-06	1.16E-04
KEGG_RENAL_CELL_CARCINOMA	Pmel1	9.80E-06	1.16E-04
KEGG_NEUROTROPHIN_SIGNALING_PATHWAY	Pmel1	1.29E-05	1.46E-04
KEGG_FOCAL_ADHESION	Pmel1	1.88E-05	2.01E-04
KEGG_AMINO_SUGAR_AND_NUCLEOTIDE_SUGAR_METABOLISM	Pmel1	3.04E-05	3.12E-04
KEGG_TOLL_LIKE_RECEPTOR_SIGNALING_PATHWAY	Pmel1	6.08E-05	5.98E-04
HALLMARK_PEROXISOME	Pmel1	6.67E-05	6.30E-04
KEGG_NOD_LIKE_RECEPTOR_SIGNALING_PATHWAY	Pmel1	1.18E-04	1.07E-03
KEGG_CHEMOKINE_SIGNALING_PATHWAY	Pmel1	1.28E-04	1.12E-03
KEGG_EPITHELIAL_CELL_SIGNALING_IN_HELICOBACTER_PYLORI_INFECTION	Pmel1	1.69E-04	1.33E-03
HALLMARK_ESTROGEN_RESPONSE_EARLY	Pmel1	1.70E-04	1.33E-03
HALLMARK_INFLAMMATORY_RESPONSE	Pmel1	1.70E-04	1.33E-03
KEGG_B_CELL_RECEPTOR_SIGNALING_PATHWAY	Pmel1	2.47E-04	1.88E-03
KEGG_REGULATION_OF_ACTIN_CYTOSKELETON	Pmel1	2.57E-04	1.89E-03
KEGG_PEROXISOME	Pmel1	2.87E-04	2.06E-03

KEGG_FC_GAMMA_R_MEDIATED_PHAGOCYTOSIS	Pmel1	6.58E-04	4.57E-03
KEGG_MAPK_SIGNALING_PATHWAY	Pmel1	7.84E-04	5.29E-03
KEGG_ENDOCYTOSIS	Pmel1	9.09E-04	5.96E-03
KEGG_PROTEASOME	Pmel1	9.72E-04	6.20E-03
HALLMARK_REACTIVE_OXIGEN_SPECIES_PATHWAY	Pmel1	1.03E-03	6.41E-03
HALLMARK_GLYCOLYSIS	Pmel1	1.35E-03	7.96E-03
HALLMARK_HYPOXIA	Pmel1	1.35E-03	7.96E-03
KEGG_NON_HOMOLOGOUS_END_JOINING	Pmel1	1.42E-03	8.18E-03
KEGG_INSULIN_SIGNALING_PATHWAY	Pmel1	2.35E-03	1.32E-02
KEGG_P53_SIGNALING_PATHWAY	Pmel1	2.77E-03	1.52E-02
HALLMARK_FATTY_ACID_METABOLISM	Pmel1	3.92E-03	2.06E-02
HALLMARK_UV_RESPONSE_UP	Pmel1	3.92E-03	2.06E-02
KEGG_NICOTINATE_AND_NICOTINAMIDE_METABOLISM	Pmel1	4.20E-03	2.15E-02
KEGG_ECM_RECEPTOR_INTERACTION	Pmel1	4.81E-03	2.42E-02
KEGG_ERBB_SIGNALING_PATHWAY	Pmel1	5.31E-03	2.61E-02
KEGG_ANTIGEN_PROCESSING_AND_PRESENTATION	Pmel1	5.66E-03	2.72E-02
KEGG_REGULATION_OF_AUTOPHAGY	Pmel1	8.79E-03	3.97E-02
KEGG_SMALL_CELL_LUNG_CANCER	OT-I	1.44E-11	3.39E-09
KEGG_GLYCOSYLPHOSPHATIDYLINOSITOL_GPI_ANCHOR_BIOSYNTHESIS	OT-I	2.58E-07	3.01E-05
KEGG_ADIPOCYTOKINE_SIGNALING_PATHWAY	OT-I	3.83E-07	3.01E-05
KEGG_RIG_I_LIKE_RECEPTOR_SIGNALING_PATHWAY	OT-I	5.12E-07	3.02E-05
KEGG_PATHWAYS_IN_CANCER	OT-I	6.51E-07	3.07E-05
KEGG_APOPTOSIS	OT-I	1.50E-06	5.89E-05
HALLMARK_PROTEIN_SECRETION	OT-I	2.30E-06	7.77E-05
KEGG_T_CELL_RECEPTOR_SIGNALING_PATHWAY	OT-I	4.12E-06	1.21E-04
KEGG_TOLL_LIKE_RECEPTOR_SIGNALING_PATHWAY	OT-I	7.61E-05	2.00E-03
HALLMARK_PI3K_AKT_MTOR_SIGNALING	OT-I	8.52E-05	2.01E-03
KEGG_UBIQUITIN_MEDIATED_PROTEOLYSIS	OT-I	2.44E-04	5.24E-03
KEGG_MAPK_SIGNALING_PATHWAY	OT-I	3.06E-04	5.68E-03
KEGG_ACUTE_MYELOID_LEUKEMIA	OT-I	3.13E-04	5.68E-03
KEGG_NOD_LIKE_RECEPTOR_SIGNALING_PATHWAY	OT-I	3.44E-04	5.81E-03
KEGG_EPITHELIAL_CELL_SIGNALING_IN_HELICOBACTER_PYLORI_INFECTION	OT-I	4.52E-04	7.11E-03
KEGG_PANCREATIC_CANCER	OT-I	4.92E-04	7.26E-03
KEGG_CHRONIC_MYELOID_LEUKEMIA	OT-I	5.57E-04	7.73E-03
KEGG_B_CELL_RECEPTOR_SIGNALING_PATHWAY	OT-I	6.02E-04	7.90E-03
KEGG_CHEMOKINE_SIGNALING_PATHWAY	OT-I	8.14E-04	1.01E-02
KEGG_PROSTATE_CANCER	OT-I	9.91E-04	1.13E-02
KEGG_FOCAL_ADHESION	OT-I	1.00E-03	1.13E-02

HALLMARK_UNFOLDED_PROTEIN_RESPONSE	OT-I	1.97E-03	2.11E-02
KEGG_SPHINGOLIPID_METABOLISM	OT-I	3.46E-03	3.55E-02
KEGG_AMINO_SUGAR_AND_NUCLEOTIDE_SUGAR_METABOLISM	OT-I	4.18E-03	4.11E-02
HALLMARK_DNA_REPAIR	OT-I	4.37E-03	4.13E-02
HALLMARK_APOPTOSIS	OT-I	5.32E-03	4.69E-02
KEGG_GLUTATHIONE_METABOLISM	OT-I	5.36E-03	4.69E-02

Table. S5 Correlation of ARID2 or PBRM1 mRNA expression level (tumor purity adjusted) to GZMB or PRF1 mRNA expression level in TCGA data.
Cor., Spearman's correlation; p, p value calculated by TIMER(*32*).

	ARID2 vs. GZMB		ARID2 vs. PRF1		PBRM1 vs. GZMB		PBRM1 vs. PRF1	
Cancer type	Cor.	p value	Cor.	p value	Cor.	p value	Cor.	p value
ACC	-0.016	8.90E-01	0.206	8.05E-02	0.15	2.04E-01	0.334	3.88E-03
BLCA	-0.326	1.42E-10	-0.277	6.25E-08	-0.277	6.79E-08	-0.228	9.69E-06
BRCA	-0.29	1.01E-20	-0.251	8.88E-16	-0.188	2.29E-09	-0.156	7.40E-07
CESC	-0.216	2.89E-04	-0.178	2.98E-03	-0.245	3.70E-05	-0.131	2.94E-02
COAD	-0.09	7.15E-02	-0.021	6.75E-01	-0.047	3.49E-01	-0.078	1.19E-01
DLBC	-0.058	7.17E-01	-0.03	8.53E-01	0.077	6.34E-01	0.077	6.31E-01
ESCA	-0.119	1.11E-01	-0.059	4.35E-01	-0.12	1.09E-01	0.036	6.34E-01
GBM	-0.191	2.52E-02	-0.189	2.73E-02	-0.148	8.47E-02	-0.115	1.81E-01
HNSC	-0.081	7.40E-02	0.07	1.22E-01	0.02	6.54E-01	0.16	3.65E-04
KICH	-0.23	6.56E-02	-0.072	5.70E-01	-0.29	1.92E-02	-0.18	1.52E-01
KIRC	-0.295	1.12E-10	-0.142	2.17E-03	-0.183	8.07E-05	-0.049	2.91E-01
KIRP	-0.108	8.36E-02	-0.074	2.37E-01	-0.139	2.54E-02	-0.06	3.40E-01
LGG	-0.122	7.65E-03	-0.074	1.06E-01	-0.044	3.38E-01	-0.003	9.46E-01
LIHC	-0.073	1.74E-01	-0.047	3.81E-01	-0.098	6.82E-02	-0.025	6.47E-01
LUAD	-0.014	7.54E-01	-0.02	6.58E-01	-0.085	5.95E-02	0.001	9.81E-01
LUSC	-0.07	1.29E-01	-0.013	7.76E-01	-0.028	5.46E-01	0.056	2.19E-01
MESO	-0.194	7.49E-02	-0.177	1.05E-01	-0.355	8.67E-04	-0.273	1.14E-02
OV	-0.227	3.14E-04	-0.215	6.55E-04	-0.268	1.77E-05	-0.186	3.20E-03
PAAD	-0.013	8.70E-01	0.092	2.32E-01	0.191	1.22E-02	0.238	1.73E-03
PCPG	-0.305	6.26E-05	-0.122	1.16E-01	-0.283	2.10E-04	0.091	2.43E-01
PRAD	-0.204	2.87E-05	-0.146	2.80E-03	-0.155	1.47E-03	-0.086	7.86E-02
READ	-0.152	7.36E-02	-0.075	3.79E-01	-0.255	2.41E-03	-0.294	4.35E-04
SARC	-0.433	1.34E-12	-0.381	7.34E-10	-0.147	2.12E-02	-0.133	3.80E-02
SKCM	-0.078	9.65E-02	0	9.95E-01	-0.083	7.46E-02	0.002	9.62E-01
STAD	-0.036	4.81E-01	0.027	6.03E-01	-0.13	1.11E-02	0.039	4.51E-01
TGCT	-0.182	2.76E-02	-0.129	1.19E-01	-0.254	2.76E-03	0.035	6.70E-01
THCA	-0.268	1.84E-09	-0.191	2.06E-05	-0.215	1.58E-06	-0.122	6.93E-03
THYM	-0.42	3.01E-06	-0.35	1.24E-04	-0.476	7.77E-08	-0.242	9.21E-03
UCEC	-0.164	4.76E-03	-0.157	6.93E-03	-0.224	1.08E-04	-0.204	4.28E-04
UVM	0.093	4.20E-01	-0.028	8.08E-01	-0.071	5.40E-01	-0.17	1.39E-01

References and Notes

1. P. Sharma, S. Hu-Lieskovan, J. A. Wargo, A. Ribas, Primary, Adaptive, and Acquired Resistance to Cancer Immunotherapy. *Cell* **168**, 707–723 (2017). doi:10.1016/j.cell.2017.01.017 Medline

2. N. Zhang, M. J. Bevan, CD8(+) T cells: Foot soldiers of the immune system. *Immunity* **35**, 161–168 (2011). doi:10.1016/j.immuni.2011.07.010 Medline

3. Y. Iwai, M. Ishida, Y. Tanaka, T. Okazaki, T. Honjo, N. Minato, Involvement of PD-L1 on tumor cells in the escape from host immune system and tumor immunotherapy by PD-L1 blockade. *Proc. Natl. Acad. Sci. U.S.A.* **99**, 12293–12297 (2002). doi:10.1073/pnas.192461099 Medline

4. A. van Elsas, A. A. Hurwitz, J. P. Allison, Combination immunotherapy of B16 melanoma using anti-cytotoxic T lymphocyte-associated antigen 4 (CTLA-4) and granulocyte/macrophage colony-stimulating factor (GM-CSF)-producing vaccines induces rejection of subcutaneous and metastatic tumors accompanied by autoimmune depigmentation. *J. Exp. Med.* **190**, 355–366 (1999). doi:10.1084/jem.190.3.355 Medline

5. S. Chen, L.-F. Lee, T. S. Fisher, B. Jessen, M. Elliott, W. Evering, K. Logronio, G. H. Tu, K. Tsaparikos, X. Li, H. Wang, C. Ying, M. Xiong, T. VanArsdale, J. C. Lin, Combination of 4-1BB agonist and PD-1 antagonist promotes antitumor effector/memory CD8 T cells in a poorly immunogenic tumor model. *Cancer Immunol. Res.* **3**, 149–160 (2015). doi:10.1158/2326-6066.CIR-14-0118 Medline

6. J. G. Doench, N. Fusi, M. Sullender, M. Hegde, E. W. Vaimberg, K. F. Donovan, I. Smith, Z. Tothova, C. Wilen, R. Orchard, H. W. Virgin, J. Listgarten, D. E. Root, Optimized sgRNA design to maximize activity and minimize off-target effects of CRISPR-Cas9. *Nat. Biotechnol.* **34**, 184–191 (2016). doi:10.1038/nbt.3437 Medline

7. W. W. Overwijk, M. R. Theoret, S. E. Finkelstein, D. R. Surman, L. A. de Jong, F. A. Vyth-Dreese, T. A. Dellemijn, P. A. Antony, P. J. Spiess, D. C. Palmer, D. M. Heimann, C. A. Klebanoff, Z. Yu, L. N. Hwang, L. Feigenbaum, A. M. Kruisbeek, S. A. Rosenberg, N. P. Restifo, Tumor regression and autoimmunity after reversal of a functionally tolerant state of self-reactive CD8+ T cells. *J. Exp. Med.* **198**, 569–580 (2003). doi:10.1084/jem.20030590 Medline

8. K. A. Hogquist, S. C. Jameson, W. R. Heath, J. L. Howard, M. J. Bevan, F. R. Carbone, T cell receptor antagonist peptides induce positive selection. *Cell* **76**, 17–27 (1994). doi:10.1016/0092-8674(94)90169-4 Medline

9. J. S. Blum, P. A. Wearsch, P. Cresswell, Pathways of antigen processing. *Annu. Rev. Immunol.* **31**, 443–473 (2013). doi:10.1146/annurev-immunol-032712-095910 Medline

10. K. S. Kobayashi, P. J. van den Elsen, NLRC5: A key regulator of MHC class I-dependent immune responses. *Nat. Rev. Immunol.* **12**, 813–820 (2012). doi:10.1038/nri3339 Medline

11. B. S. Parker, J. Rautela, P. J. Hertzog, Antitumour actions of interferons: Implications for cancer therapy. *Nat. Rev. Cancer* **16**, 131–144 (2016). doi:10.1038/nrc.2016.14 Medline

12. J. Gao, L. Z. Shi, H. Zhao, J. Chen, L. Xiong, Q. He, T. Chen, J. Roszik, C. Bernatchez, S. E. Woodman, P.-L. Chen, P. Hwu, J. P. Allison, A. Futreal, J. A. Wargo, P. Sharma, Loss of IFN-γ Pathway Genes in Tumor Cells as a Mechanism of Resistance to Anti-CTLA-4 Therapy. *Cell* **167**, 397–404.e9 (2016). doi:10.1016/j.cell.2016.08.069 Medline

13. J. M. Zaretsky, A. Garcia-Diaz, D. S. Shin, H. Escuin-Ordinas, W. Hugo, S. Hu-Lieskovan, D. Y. Torrejon, G. Abril-Rodriguez, S. Sandoval, L. Barthly, J. Saco, B. Homet Moreno, R. Mezzadra, B. Chmielowski, K. Ruchalski, I. P. Shintaku, P. J. Sanchez, C. Puig-Saus, G. Cherry, E. Seja, X. Kong, J. Pang, B. Berent-Maoz, B. Comin-Anduix, T. G. Graeber, P. C. Tumeh, T. N. M. Schumacher, R. S. Lo, A. Ribas, Mutations Associated with Acquired Resistance to PD-1 Blockade in Melanoma. *N. Engl. J. Med.* **375**, 819–829 (2016). doi:10.1056/NEJMoa1604958 Medline

14. R. T. Manguso, H. W. Pope, M. D. Zimmer, F. D. Brown, K. B. Yates, B. C. Miller, N. B. Collins, K. Bi, M. W. LaFleur, V. R. Juneja, S. A. Weiss, J. Lo, D. E. Fisher, D. Miao, E. Van Allen, D. E. Root, A. H. Sharpe, J. G. Doench, W. N. Haining, In vivo CRISPR screening identifies Ptpn2 as a cancer immunotherapy target. *Nature* **547**, 413–418 (2017). doi:10.1038/nature23270 Medline

15. K. G. Patel, J. R. Swartz, Surface functionalization of virus-like particles by direct conjugation using azide-alkyne click chemistry. *Bioconjug. Chem.* **22**, 376–387 (2011). doi:10.1021/bc100367u Medline

16. H. Dong, G. Zhu, K. Tamada, L. Chen, B7-H1, a third member of the B7 family, co-stimulates T-cell proliferation and interleukin-10 secretion. *Nat. Med.* **5**, 1365–1369 (1999). doi:10.1038/70932 Medline

17. G. J. Freeman, A. J. Long, Y. Iwai, K. Bourque, T. Chernova, H. Nishimura, L. J. Fitz, N. Malenkovich, T. Okazaki, M. C. Byrne, H. F. Horton, L. Fouser, L. Carter, V. Ling, M. R. Bowman, B. M. Carreno, M. Collins, C. R. Wood, T. Honjo, Engagement of the PD-1 immunoinhibitory receptor by a novel B7 family member leads to negative regulation of lymphocyte activation. *J. Exp. Med.* **192**, 1027–1034 (2000). doi:10.1084/jem.192.7.1027 Medline

18. M. Kleppe, J. Soulier, V. Asnafi, N. Mentens, T. Hornakova, L. Knoops, S. Constantinescu, F. Sigaux, J. P. Meijerink, P. Vandenberghe, M. Tartaglia, R. Foa, E. Macintyre, T. Haferlach, J. Cools, PTPN2 negatively regulates oncogenic JAK1 in T-cell acute lymphoblastic leukemia. *Blood* **117**, 7090–7098 (2011). doi:10.1182/blood-2010-10-314286 Medline

19. D. Kaiserman, P. I. Bird, Control of granzymes by serpins. *Cell Death Differ.* **17**, 586–595 (2010). doi:10.1038/cdd.2009.169 Medline

20. N. Ratner, S. J. Miller, A RASopathy gene commonly mutated in cancer: The neurofibromatosis type 1 tumour suppressor. *Nat. Rev. Cancer* **15**, 290–301 (2015). doi:10.1038/nrc3911 Medline

21. S. Messina, L. Frati, C. Leonetti, C. Zuchegna, E. Di Zazzo, A. Calogero, A. Porcellini, Dual-specificity phosphatase DUSP6 has tumor-promoting properties in human glioblastomas. *Oncogene* **30**, 3813–3820 (2011). doi:10.1038/onc.2011.99 Medline

22. T. N. Phoenix, S. Temple, Spred1, a negative regulator of Ras-MAPK-ERK, is enriched in CNS germinal zones, dampens NSC proliferation, and maintains ventricular zone structure. *Genes Dev.* **24**, 45–56 (2010). doi:10.1101/gad.1839510 Medline

23. R. Arafeh, N. Qutob, R. Emmanuel, A. Keren-Paz, J. Madore, A. Elkahloun, J. S. Wilmott, J. J. Gartner, A. Di Pizio, S. Winograd-Katz, S. Sindiri, R. Rotkopf, K. Dutton-Regester, P. Johansson, A. L. Pritchard, N. Waddell, V. K. Hill, J. C. Lin, Y. Hevroni, S. A. Rosenberg, J. Khan, S. Ben-Dor, M. Y. Niv, I. Ulitsky, G. J. Mann, R. A. Scolyer, N. K. Hayward, Y. Samuels, Recurrent inactivating RASA2 mutations in melanoma. *Nat. Genet.* **47**, 1408–1410 (2015). doi:10.1038/ng.3427 Medline

24. G. Li, W. Ci, S. Karmakar, K. Chen, R. Dhar, Z. Fan, Z. Guo, J. Zhang, Y. Ke, L. Wang, M. Zhuang, S. Hu, X. Li, L. Zhou, X. Li, M. F. Calabrese, E. R. Watson, S. M. Prasad, C. Rinker-Schaeffer, S. E. Eggener, T. Stricker, Y. Tian, B. A. Schulman, J. Liu, K. P. White, SPOP promotes tumorigenesis by acting as a key regulatory hub in kidney cancer. *Cancer Cell* **25**, 455–468 (2014). doi:10.1016/j.ccr.2014.02.007 Medline

25. D. T. Frederick, A. Piris, A. P. Cogdill, Z. A. Cooper, C. Lezcano, C. R. Ferrone, D. Mitra, A. Boni, L. P. Newton, C. Liu, W. Peng, R. J. Sullivan, D. P. Lawrence, F. S. Hodi, W. W. Overwijk, G. Lizée, G. F. Murphy, P. Hwu, K. T. Flaherty, D. E. Fisher, J. A. Wargo, BRAF inhibition is associated with enhanced melanoma antigen expression and a more favorable tumor microenvironment in patients with metastatic melanoma. *Clin. Cancer Res.* **19**, 1225–1231 (2013). doi:10.1158/1078-0432.CCR-12-1630 Medline

26. P. J. R. Ebert, J. Cheung, Y. Yang, E. McNamara, R. Hong, M. Moskalenko, S. E. Gould, H. Maecker, B. A. Irving, J. M. Kim, M. Belvin, I. Mellman, MAP Kinase Inhibition Promotes T Cell and Anti-tumor Activity in Combination with PD-L1 Checkpoint Blockade. *Immunity* **44**, 609–621 (2016). doi:10.1016/j.immuni.2016.01.024 Medline

27. R. C. Koya, S. Mok, N. Otte, K. J. Blacketor, B. Comin-Anduix, P. C. Tumeh, A. Minasyan, N. A. Graham, T. G. Graeber, T. Chodon, A. Ribas, BRAF inhibitor vemurafenib improves the antitumor activity of adoptive cell immunotherapy. *Cancer Res.* **72**, 3928–3937 (2012). doi:10.1158/0008-5472.CAN-11-2837 Medline

28. C. Kadoch, G. R. Crabtree, Mammalian SWI/SNF chromatin remodeling complexes and cancer: Mechanistic insights gained from human genomics. *Sci. Adv.* **1**, e1500447 (2015). doi:10.1126/sciadv.1500447 Medline

29. B. Lemon, C. Inouye, D. S. King, R. Tjian, Selectivity of chromatin-remodelling cofactors for ligand-activated transcription. *Nature* **414**, 924–928 (2001). doi:10.1038/414924a Medline

30. Q. Zhang, M. J. Lenardo, D. Baltimore, 30 Years of NF-κB: A Blossoming of Relevance to Human Pathobiology. *Cell* **168**, 37–57 (2017). doi:10.1016/j.cell.2016.12.012 Medline

31. Y. Sancak, L. Bar-Peled, R. Zoncu, A. L. Markhard, S. Nada, D. M. Sabatini, Ragulator-Rag complex targets mTORC1 to the lysosomal surface and is necessary for its activation by amino acids. *Cell* **141**, 290–303 (2010). doi:10.1016/j.cell.2010.02.024 Medline

32. B. Li, E. Severson, J.-C. Pignon, H. Zhao, T. Li, J. Novak, P. Jiang, H. Shen, J. C. Aster, S. Rodig, S. Signoretti, J. S. Liu, X. S. Liu, Comprehensive analyses of tumor immunity:

Implications for cancer immunotherapy. *Genome Biol.* **17**, 174 (2016). doi:10.1186/s13059-016-1028-7 Medline

33. C. Kadoch, R. T. Williams, J. P. Calarco, E. L. Miller, C. M. Weber, S. M. G. Braun, J. L. Pulice, E. J. Chory, G. R. Crabtree, Dynamics of BAF-Polycomb complex opposition on heterochromatin in normal and oncogenic states. *Nat. Genet.* **49**, 213–222 (2017). doi:10.1038/ng.3734 Medline

34. Z. Yan, K. Cui, D. M. Murray, C. Ling, Y. Xue, A. Gerstein, R. Parsons, K. Zhao, W. Wang, PBAF chromatin-remodeling complex requires a novel specificity subunit, BAF200, to regulate expression of selective interferon-responsive genes. *Genes Dev.* **19**, 1662–1667 (2005). doi:10.1101/gad.1323805 Medline

35. J. R. Groom, A. D. Luster, CXCR3 ligands: Redundant, collaborative and antagonistic functions. *Immunol. Cell Biol.* **89**, 207–215 (2011). doi:10.1038/icb.2010.158 Medline

36. I. Varela, P. Tarpey, K. Raine, D. Huang, C. K. Ong, P. Stephens, H. Davies, D. Jones, M. L. Lin, J. Teague, G. Bignell, A. Butler, J. Cho, G. L. Dalgliesh, D. Galappaththige, C. Greenman, C. Hardy, M. Jia, C. Latimer, K. W. Lau, J. Marshall, S. McLaren, A. Menzies, L. Mudie, L. Stebbings, D. A. Largaespada, L. F. Wessels, S. Richard, R. J. Kahnoski, J. Anema, D. A. Tuveson, P. A. Perez-Mancera, V. Mustonen, A. Fischer, D. J. Adams, A. Rust, W. Chan-on, C. Subimerb, K. Dykema, K. Furge, P. J. Campbell, B. T. Teh, M. R. Stratton, P. A. Futreal, Exome sequencing identifies frequent mutation of the SWI/SNF complex gene PBRM1 in renal carcinoma. *Nature* **469**, 539–542 (2011). doi:10.1038/nature09639 Medline

37. D. Miao *et al*., Genomic correlates of response to immune checkpoint therapies in clear cell renal cell carcinoma. *Science* (2017).

38. E. Hodis, I. R. Watson, G. V. Kryukov, S. T. Arold, M. Imielinski, J.-P. Theurillat, E. Nickerson, D. Auclair, L. Li, C. Place, D. Dicara, A. H. Ramos, M. S. Lawrence, K. Cibulskis, A. Sivachenko, D. Voet, G. Saksena, N. Stransky, R. C. Onofrio, W. Winckler, K. Ardlie, N. Wagle, J. Wargo, K. Chong, D. L. Morton, K. Stemke-Hale, G. Chen, M. Noble, M. Meyerson, J. E. Ladbury, M. A. Davies, J. E. Gershenwald, S. N. Wagner, D. S. B. Hoon, D. Schadendorf, E. S. Lander, S. B. Gabriel, G. Getz, L. A. Garraway, L. Chin, A landscape of driver mutations in melanoma. *Cell* **150**, 251–263 (2012). doi:10.1016/j.cell.2012.06.024 Medline

39. S. Chen, N. E. Sanjana, K. Zheng, O. Shalem, K. Lee, X. Shi, D. A. Scott, J. Song, J. Q. Pan, R. Weissleder, H. Lee, F. Zhang, P. A. Sharp, Genome-wide CRISPR screen in a mouse model of tumor growth and metastasis. *Cell* **160**, 1246–1260 (2015). doi:10.1016/j.cell.2015.02.038 Medline

40. W. Li, H. Xu, T. Xiao, L. Cong, M. I. Love, F. Zhang, R. A. Irizarry, J. S. Liu, M. Brown, X. S. Liu, MAGeCK enables robust identification of essential genes from genome-scale CRISPR/Cas9 knockout screens. *Genome Biol.* **15**, 554 (2014). doi:10.1186/s13059-014-0554-4 Medline

41. M. I. Love, W. Huber, S. Anders, Moderated estimation of fold change and dispersion for RNA-seq data with DESeq2. *Genome Biol.* **15**, 550 (2014). doi:10.1186/s13059-014-0550-8 Medline

42. C. Trapnell, B. A. Williams, G. Pertea, A. Mortazavi, G. Kwan, M. J. van Baren, S. L. Salzberg, B. J. Wold, L. Pachter, Transcript assembly and quantification by RNA-Seq reveals unannotated transcripts and isoform switching during cell differentiation. *Nat. Biotechnol.* **28**, 511–515 (2010). doi:10.1038/nbt.1621 Medline

43. J. D. Buenrostro, B. Wu, H. Y. Chang, W. J. Greenleaf, ATAC-seq: A Method for Assaying Chromatin Accessibility Genome-Wide. *Curr. Protoc. Mol. Biol.* **109**, 1–9 (2015). doi:10.1002/0471142727.mb2129s109 Medline

44. J. D. Buenrostro, P. G. Giresi, L. C. Zaba, H. Y. Chang, W. J. Greenleaf, Transposition of native chromatin for fast and sensitive epigenomic profiling of open chromatin, DNA-binding proteins and nucleosome position. *Nat. Methods* **10**, 1213–1218 (2013). doi:10.1038/nmeth.2688 Medline

45. H. Li, R. Durbin, Fast and accurate short read alignment with Burrows-Wheeler transform. *Bioinformatics* **25**, 1754–1760 (2009). doi:10.1093/bioinformatics/btp324 Medline

46. Y. Zhang, T. Liu, C. A. Meyer, J. Eeckhoute, D. S. Johnson, B. E. Bernstein, C. Nusbaum, R. M. Myers, M. Brown, W. Li, X. S. Liu, Model-based analysis of ChIP-Seq (MACS). *Genome Biol.* **9**, R137 (2008). doi:10.1186/gb-2008-9-9-r137 Medline

47. S. Wang, H. Sun, J. Ma, C. Zang, C. Wang, J. Wang, Q. Tang, C. A. Meyer, Y. Zhang, X. S. Liu, Target analysis by integration of transcriptome and ChIP-seq data with BETA. *Nat. Protoc.* **8**, 2502–2515 (2013). doi:10.1038/nprot.2013.150 Medline

48. A. Subramanian, P. Tamayo, V. K. Mootha, S. Mukherjee, B. L. Ebert, M. A. Gillette, A. Paulovich, S. L. Pomeroy, T. R. Golub, E. S. Lander, J. P. Mesirov, Gene set enrichment analysis: A knowledge-based approach for interpreting genome-wide expression profiles. *Proc. Natl. Acad. Sci. U.S.A.* **102**, 15545–15550 (2005). doi:10.1073/pnas.0506580102 Medline

49. V. K. Mootha, C. M. Lindgren, K.-F. Eriksson, A. Subramanian, S. Sihag, J. Lehar, P. Puigserver, E. Carlsson, M. Ridderstråle, E. Laurila, N. Houstis, M. J. Daly, N. Patterson, J. P. Mesirov, T. R. Golub, P. Tamayo, B. Spiegelman, E. S. Lander, J. N. Hirschhorn, D. Altshuler, L. C. Groop, PGC-1alpha-responsive genes involved in oxidative phosphorylation are coordinately downregulated in human diabetes. *Nat. Genet.* **34**, 267–273 (2003). doi:10.1038/ng1180 Medline

50. S. Heinz, C. Benner, N. Spann, E. Bertolino, Y. C. Lin, P. Laslo, J. X. Cheng, C. Murre, H. Singh, C. K. Glass, Simple combinations of lineage-determining transcription factors prime cis-regulatory elements required for macrophage and B cell identities. *Mol. Cell* **38**, 576–589 (2010). doi:10.1016/j.molcel.2010.05.004 Medline